

AD-A252 177



2

NAVAL POSTGRADUATE SCHOOL  
Monterey, California



DTIC  
ELECTE  
JUN 29 1992  
S B D

THESIS

THE EFFECT OF THERMOMECHANICAL  
PROCESSING PARAMETERS ON THE AMBIENT  
BEHAVIOR OF 10% VOLUME 6061 AL-ALUMINA

by

David F. Eastwood Jr.

March, 1992

Thesis Advisors:

T. R. McNelly

Co-Advisor:

P. N. Kalu

Approved for public release; distribution is unlimited.

92-16883



92 6 26 013

Unclassified

SECURITY CLASSIFICATION OF THIS PAGE

REPORT DOCUMENTATION PAGE				Form Approved OMB No 0704-0188	
1a REPORT SECURITY CLASSIFICATION <b>Unclassified</b>		1b RESTRICTIVE MARKINGS			
2a SECURITY CLASSIFICATION AUTHORITY		3 DISTRIBUTION / AVAILABILITY OF REPORT			
3b DECLASSIFICATION / DOWNGRADING SCHEDULE					
4 PERFORMING ORGANIZATION REPORT NUMBER(S)		5 MONITORING ORGANIZATION REPORT NUMBER(S)			
6a NAME OF PERFORMING ORGANIZATION <b>Naval Postgraduate School</b>	6b OFFICE SYMBOL (if applicable) <b>34</b>	7a NAME OF MONITORING ORGANIZATION <b>Naval Postgraduate School</b>			
6c ADDRESS (City, State, and ZIP Code) <b>Monterey, Ca 93943-5000</b>		7b ADDRESS (City, State, and ZIP Code) <b>Monterey, Ca 93943-5000</b>			
8a NAME OF FUNDING / SPONSORING ORGANIZATION	8b OFFICE SYMBOL (if applicable)	9 PROCUREMENT INSTRUMENT IDENTIFICATION NUMBER			
8c ADDRESS (City, State, and ZIP Code)		10 SOURCE OF FUNDING NUMBERS			
		PROGRAM ELEMENT NO	PROJECT NO	TASK NO	WORK UNIT ACCESSION NO
11 TITLE (Include Security Classification) <b>The Effect of Thermomechanical Processing Parameters on the Ambient Behavior of 10% Volume 6061 Al-Alumina</b>					
12 PERSONAL AUTHOR(S) <b>David F. Eastwood Jr.</b>					
13a TYPE OF REPORT <b>Master's Thesis</b>	13b TIME COVERED FROM _____ TO _____	14 DATE OF REPORT (Year, Month, Day) <b>March 1992</b>	15 PAGE COUNT <b>85</b>		
16 SUPPLEMENTARY NOTATION <b>The views expressed in this thesis are those of the author and do not reflect official policy or position of the Department of Defense or U. S. Government</b>					
17 COSATI CODES			18 SUBJECT TERMS (Continue on reverse if necessary and identify by block number)  <b>Cast Metal Matrix Composite, Particulate, Processing, Ductility, Aging</b>		
FIELD	GROUP	SUB-GROUP			
19 ABSTRACT (Continue on reverse if necessary and identify by block number)  Thermomechanical Processing was conducted on a 10 vol. pct. 6061 Alumina particle reinforced 'metal matrix composite' (MMC). The TMP employed consisted of isothermal rolling with intermediate annealing, using a schedule of reduction with constrain strain per pass. The as-processed material exhibited high strength while simultaneously achieving ductility comparable to that of the unreinforced 6061 matrix alloy. In the fully annealed condition, the composite's strength and ductility were essentially equal to those of the unreinforced aluminum. An aging study showed accelerated aging and greater peak strength for the composite. Finally, a process and heat treatment combination was established in an attempt to optimize simultaneously the strength and ductility of the composite. It was found that the composite could be aged to a peak strength of 340 MPA while retaining a ductility of 14 percent elongation to failure.					
20 DISTRIBUTION / AVAILABILITY OF ABSTRACT <input checked="" type="checkbox"/> UNCLASSIFIED/UNLIMITED <input type="checkbox"/> SAME AS RPT <input type="checkbox"/> DTIC USERS			21 ABSTRACT SECURITY CLASSIFICATION <b>Unclassified</b>		
22a NAME OF RESPONSIBLE INDIVIDUAL <b>T. R. McNeley</b>		22b TELEPHONE (include Area Code) <b>(408)646-2589</b>	22c OFFICE SYMBOL <b>69MC</b>		

Approved for public release; distribution is unlimited.

**The Effect of Secondary Thermomechanical Processing Parameters on the Ambient  
Temperature Behavior of 10% Volume 6061 Al-Alumina Metal Matrix Composite**

by

**David F. Eastwood Jr.**  
Lieutenant, United States Navy  
B.A., The University of California, Berkeley, 1984

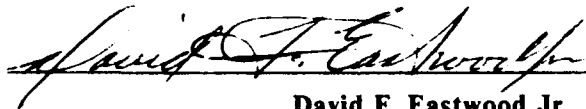
Submitted in partial fulfillment  
of the requirements for the degree of

**MASTER OF SCIENCE IN MECHANICAL ENGINEERING**

from the

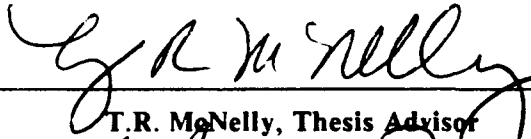
**NAVAL POSTGRADUATE SCHOOL**  
March 1992

Author:



**David F. Eastwood Jr.**

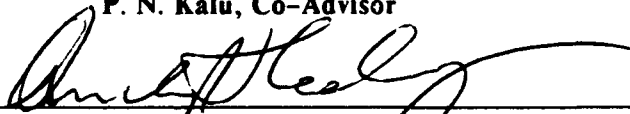
Approved by:



**T.R. McNelly, Thesis Advisor**



**P. N. Kalu, Co-Advisor**



**Anthony J. Healy, Chairman,  
Department of Mechanical Engineering**

## ABSTRACT

Thermomechanical processing (TMP) was conducted on a 10 volume percent, 6061 Al-Al<sub>2</sub>O<sub>3</sub> particle reinforced 'metal-matrix composite' (MMC). The TMP employed consisted of isothermal rolling with intermediate annealing using a schedule of reduction with constant strain per pass for most of the schedule. The as-processed material exhibited high strength while simultaneously achieving ductility comparable to that of the unreinforced 6061 matrix alloy. In the fully annealed condition, the composite's strength and ductility were essentially equal to those of the unreinforced aluminum. An aging study showed accelerated aging and greater peak strength for the composite. Finally, a process and heat treatment combination was established in an attempt to optimize simultaneously the strength and ductility of the composite. It was found that the composite could be aged to a peak strength of 340 MPA while retaining a ductility of 14 percent elongation to failure.



<b>Accession For</b>	
NTIS GRA&I	<input checked="" type="checkbox"/>
DTIC TAB	<input type="checkbox"/>
Unannounced	<input type="checkbox"/>
Justification	
By _____	
Distribution/	
<b>Availability Codes</b>	
<b>Dist</b>	<b>Avail and/or Special</b>
A-1	

## TABLE OF CONTENTS

<b>I. INTRODUCTION</b> .....	1
<b>A. HISTORICAL PERSPECTIVE</b> .....	1
<b>II BACKGROUND</b> .....	6
<b>A. EARLY WORK IN SUPERPLASTICITY</b> .....	6
<b>B. COMPOSITES</b> .....	7
<b>III EXPERIMENTAL PROCEDURE</b> .....	9
<b>A. AS RECEIVED MATERIAL AND INITIAL PROCESSING</b> .....	9
<b>B. ROLLING</b> .....	10
<b>C. MACHINING OF TENSILE COUPONS</b> .....	13
<b>D. TENSILE TESTING</b> .....	14
<b>E. AGING STUDY</b> .....	14
<b>F. OPTICAL MICROSCOPY</b> .....	16
<b>G. SCANNING ELECTRON MICROSCOPE (SEM)</b> .....	17
<b>IV. THEORETICAL PRESENTATION</b> .....	18
<b>A. THE EFFECT OF SECONDARY TMP ON MICROSTRUCTURE</b> .....	18
<b>B. UNREINFORCED MATRIX</b> .....	18
<b>C. COMPOSITE</b> .....	23

<b>V. RESULTS AND DISCUSSION</b> .....	<b>30</b>
<b>A. EFFECT OF PROCESSING ON MICROSTRUCTURE</b> .....	<b>30</b>
<b>B. TENSILE TEST RESULTS</b> .....	<b>45</b>
<b>C. TOTAL STRAIN</b> .....	<b>57</b>
<b>D. AGING STUDY</b> .....	<b>57</b>
<b>E. OPTIMIZATION</b> .....	<b>60</b>
<b>VI. LIST OF REFERENCES</b> .....	<b>76</b>
<b>VII. INITIAL DISTRIBUTION LIST</b> .....	<b>81</b>

## I. INTRODUCTION

### A. HISTORICAL PERSPECTIVE

#### 1. DEFINITIONS:

The term "metal matrix composite" (MMC) is defined so as to distinguish this class of materials from the more general classes of multi-phase or polycrystalline metallic materials. The following criteria must be met if a material is to be considered a MMC.

- It must be man-made.
- It must be a combination of at least two chemically distinct materials with a distinct interface separating the constituents.
- The separate materials forming the composite must be combined three-dimensionally. (Laminates such as clad metals or honeycomb sandwiches are not considered basic composite materials if the same metal is used throughout.)
- It should be created to obtain properties which would not otherwise be achieved by any of the individual constituents. [Ref. 1]

Metal Matrix composites are generally divided into three broad categories based on both size and geometry of the reinforcement:

- *particle-reinforced;*
- *continuous fiber-reinforced;*
- *whisker-reinforced.*

Further, each category is broadly defined as follows.

- *Particle-reinforced* The composite is characterized by dispersed particles of greater than  $1.0\mu\text{m}$  in size with volume fractions of 5 to 40%. A closely related category of materials is dispersion strengthened metals, which are characterized by a microstructure consisting of an alloyed matrix within which fine particles are uniformly dispersed; however, for the dispersion strengthened metals, the particle diameter ranges from about  $0.01$  to  $0.1\mu\text{m}$  and the volume fraction of particles ranges from 1 to 15%. The inclusion of the particles results in a dramatic increase in the yield stress and/or the work hardening rate. The intrinsic properties of the reinforcement particles (i.e., the high elastic modulus) are not utilized. The principal function of the particles is to impede the the movement of dislocations. [Ref. 2]
- *Continuous fiber-reinforced* The composite contains fibers which run the length and/or the breath of the material and serve as the primary load bearing component of the material. Therefore, the fiber's load bearing capacity is of prime importance in the selection criteria.
- *Whisker-reinforced* The reinforcement consists of a discontinuous phase of fibrous nature, oriented randomly throughout the metal and with a size range from  $0.1$  to  $250\mu\text{m}$ . The volume fraction varies from a few percent to greater than 70%. [Ref. 3]

The properties of each type or reinforcement is listed in Table 1.

The as-received material studied in this project was a particulate MMC and consisted of a 10 volume percent particulate alumina ( $\text{Al}_2\text{O}_3$ ) in a matrix of 6061 aluminum. The material had been cast and subsequently extruded by the manufacturer utilizing a reduction ratio of 17:1, corresponding to a total strain of 2.8 at a temperature of  $\approx 500^\circ\text{C}$ . Optical microscopy determined that the average individual particle diameter in the as-received material was  $\approx 12\mu\text{m}$  with the particles in clusters and bands throughout the material.

**Table 1. BASIC PROPERTIES OF PARTICULATE AND FIBER REINFORCEMENT [Ref. 4]**

	Particulate Hardening	Fiber Reinforcement
Role of Matrix	Principal load-bearing component	Medium for transferring load to the fibers
Matrix Work Hardening	Major hardening mechanism; work hardening rate depends on the particle forms and the spacing between them	Minor hardening factor
Role of the Dispersed Phase	Impedes the dislocation movement	Principal load-bearing component; obstruction of dislocation movement by indirect means is of secondary importance

## 2. COMPOSITE PRODUCTION

The development of the three types of MMC's has occurred over the last few decades with the initial interest as well as the early successes occurring in the area of continuous filament MMC's primarily for aerospace and military applications. During this same period, the discontinuous MMC's were plagued by inherent problems associated with fabrication. The most notable of these fabrication problems were high cost, poor reproducibility, low fracture toughness and an unacceptably low ductility. They could be said to exhibit poor fabricability. In recent years, there has been a renewed interest in development of discontinuous MMC's due to advances in fabrication methods and development of lower-cost, more reliable production techniques [Ref. 5].

### 3. REINFORCEMENT INTRODUCTION INTO MATRIX

There are several routes for introducing the reinforcement ceramic to the matrix, each of which has distinct advantages and disadvantages. The final microstructure and properties of the composite material is a function of the processing method, type, as well as quantity of the reinforcing particles.

- *POWDER METALLURGY* This method offers the most flexibility in terms of alloy chemistry, particle size and volume fraction.
- *INGOT METALLURGY* An example of this type of production is stir casting. It has the disadvantage of particle aggregation which limits the volume fraction of the ceramic which can be incorporated and reactivity of the reinforcement with the molten metal must be explored.
- *SPRAY CASTING* Although less susceptible to reactivity problems, the size range and volume fraction of ceramic particles is still limited. [Ref. 6]

### 4. ADVANTAGES OF PARTICULATE MMC'S

All MMC's types display several generic advantages which make them very appealing for use in a wide variety of engineering applications. The relative magnitude of each type of advantage is a function of the MMC type, processing and reinforcement; however, most MMC's include a combination of the following:

- high strength;
- high elastic modulus;
- low sensitivity to temperature changes or thermal shock;
- high surface durability and low sensitivity to surface flaws;

- high electrical and thermal conductivity. [Ref. 7]

Discontinuous MMC's are abundant since most are fabricated from common refractory fibers. The cost of discontinuous fiber and particulate reinforcement is inexpensive in comparison to continuous fiber reinforcement with discontinuous  $\text{Al}_2\text{O}_3$  costing 35-90 \$/Kg to 165-330 \$/Kg for the corresponding continuous fiber reinforcement [Ref. 8]. Also, discontinuous MMC's possess important commercial fabrication advantages for, unlike fiber reinforced MMC's, they can be mechanically processed using the same techniques and equipment developed for unreinforced alloys such as forging, extrusion, etc. Also, they possess more nearly isotropic properties if the particle dispersion is random in the matrix.

## II BACKGROUND

### A. EARLY WORK IN SUPERPLASTICITY

#### 1. EARLY SUCCESSES

Since the mid-1980's, research has been on-going at the Naval Postgraduate School in the area of superplasticity in Al-Mg alloys. This research has achieved superplastic ductilities of over 1000 percent elongation at a relatively low temperature of 300°C. This greatly enhanced ductility has been shown to be a result of TMP which included controlled isothermal rolling with a controlled reduction schedule and annealing intervals between all rolling passes.

#### 2. SUPER PLASTIC MICROSTRUCTURE

Recent work by T. E. Gorsuch [Ref. 9] determined the primary microstructural effects of the TMP which promoted superplasticity. The effects isolated were a thorough redistribution of the  $\beta$  ( $Mg_5Al_8$ ) precipitate particles throughout the material and the formation of very fine grains. The fine grains were determined to result in 'particle stimulated nucleation' of recrystallization during the controlled anneals. Uniformly distributed second-phase particles helped to nucleate new grains as well as simultaneously provided a well dispersed phase which impeded further grain growth. A series of papers has been published in this area, and the

success with superplasticity and lessons learned from research were subsequently applied to the composite arena. Similar TMP was adapted in the present study.

## **B. COMPOSITES**

### **1. COMPOSITE DUCTILITY ENHANCEMENT**

The first attempt to apply these lessons of microstructural control to discontinuous, particulate reinforced composites was explored by T. A. Schaefer [Ref. 10] with a cast, 10 volume percent Al-Al<sub>2</sub>O<sub>3</sub> material at ambient temperature. The principal results of this initial study demonstrated that extrusion significantly improved strength and ductility over the as cast condition. Additional secondary TMP further improved both the strength and ductility of rolled material when compared to the as-received, extruded material. The improvements in mechanical behavior were shown to be the consequence of the improved homogeneity of the ceramic particle distribution, and the refinement of the matrix grain structure. The application of the TMP did not cause any microstructural damage during processing contrary to studies involving fiber-reinforced composites. Lastly, a preliminary study explored the aging response of the composite, revealing that the composite showed accelerated age hardenability to an increased peak strength while still exhibiting high ductility compared to the as-received, extruded condition.

## 2. ELEVATED TEMPERATURE RESEARCH

Work by P. Macri [Ref. 11], M. Magill [Ref. 12] and later by T. Schauder [Ref. 13] explored the elevated temperature response of the same 10 volume percent Al-Al<sub>2</sub>O<sub>3</sub> composite. Their results demonstrated that while, at low temperatures, the Al<sub>2</sub>O<sub>3</sub> particles greatly influenced the mechanical behavior, as temperature increased, the matrix had an increasingly dominant role in the overall mechanical response of the material.

## 3. THESIS CONTRIBUTIONS TO PREVIOUS FINDINGS

As mentioned, the results of the earlier work done by Schaefer et al. serves as an embarkation point for this thesis. This current study also serves to expand the research to the following areas: temperature dependence of the microstructural development, post-rolling heat treatments, a more complete aging response study, and an initial attempt at optimization of the mechanical properties of the composite. Unreinforced 6061 aluminum was identically processed as a control material. This was done to separate particle and matrix interaction from the purely matrix effects. Additional areas of research included studying the effect of a pre-rolling solution treatment, particle stimulated nucleation (PSN) effects, grain refinement effects, and composition analysis utilizing the scanning electron microscope (SEM).

### III EXPERIMENTAL PROCEDURE

#### A. AS RECEIVED MATERIAL AND INITIAL PROCESSING

##### 1. CASTING

Initial casting of the particulate composite was performed by the manufacturer, Dural Aluminum Composites Corporation (DURALCAN) of San Diego, Ca. The 6061 Al-Al<sub>2</sub>O<sub>3</sub> 'metal matrix composite' (MMC) contained 10 volume percentage alumina particles with an individual mean particle diameter of  $\approx 12\mu\text{m}$ .

##### 2. EXTRUSION

After initial consolidation by casting, a hot extrusion was conducted by the manufacturer to shape the material and improve the microstructure and mechanical properties of the composite. The extrusion was performed at a ratio of 17:1, corresponding to a true strain of 2.8 and yielded a round-cornered bar with the nominal dimensions of 19 mm (0.748") thick and 76 mm (2.99") wide.[Ref. 14] The bars were further sectioned using a power hack saw (Racine, Sandvik High Speed Blade, Tapomatic #2 Cutting Fluid). The final billets were 72.4 mm (2.85") wide, 23.9 mm (0.94") long and 19 mm (0.748") thick, each being rounded along its edges.

### 3. SOLUTION TREATMENT

In an effort to determine the effect of solution treatment prior to rolling, one set of samples was solution treated while a second set was not solution treated. Solution treatments were conducted for a duration of 90 minutes at a temperature of 560° C using a Stabil-Glow Blue M Box Type furnace.

### B. ROLLING

#### 1. PROCEDURE

Similar rolling schedules were conducted on both the composite and unreinforced 6061 aluminum for two separate temperatures (350° C and 500° C). The rolling schedules were prepared to obtain approximately constant strain per pass, (10% reduction for the first three passes increasing to 30% reduction for subsequent passes) with a 30 minute anneal performed between all passes. The intermediate anneal was conducted at processing temperature of the material. Upon exiting the final rolling pass, the material was immediately water quenched. Samples were sectioned from roll passes #8 and #9, corresponding to rolling strains of approximately 2.4 and 2.8 respectively. The material was then fabricated into coupons for tensile and hardness testing. Silicone lubricant was applied to the mill rolling surface on all 30% reduction passes to prevent sticking between the roller face and the material.

## 2. CALCULATIONS

The rolling mill deflection on each pass was calculated as the difference between the roller gap setting and the exit thickness of the sample.

The engineering strain (reduction) was determined by the following equation:

$$\epsilon = \frac{T_0 - T_f}{T_0} \quad (1)$$

In equation (1) above,  $\epsilon$  (epsilon) is the engineering strain,  $T_0$  is the original thickness, and  $T_f$  is the final thickness.

The true strain (reduction) equation was determined as follows:

$$\epsilon_{\text{true}} = \ln(1 + \epsilon) \quad (2)$$

The corresponding strain rate on each rolling pass was determined following Dieter according to the equation: [Ref. 15]

$$\dot{\epsilon} = \frac{V_r}{\sqrt{R h_0}} \sqrt{\epsilon(1 + \epsilon/4)} \quad (3)$$

For the equation above,  $V_r = 2 \cdot \pi \cdot R \cdot n$  (in/sec),  $n$  = speed of the roller (rev/sec),  $R$  = Roller radius (in),  $h_0$  = initial sample thickness (in), and  $\epsilon$  = strain as defined in equation (1).

### 3. SCHEDULES

A representative rolling schedule is provided below with the full set of schedules listed in the appendix. The strain listed is the true strain as defined in equation (2). The true strain at rolls #8 and #9 are listed to show cumulative reduction for both sample thicknesses used for tensile tests.

Table 2. 350°C PROCESSED ALUMINA COMPOSITE ROLLING SCHEDULE

Roll #	$T_o$ (in)	$T_f$ (in)	Mill Gap Setting (in)	Mill Deflect. (in)	$\dot{\epsilon}$ (1/sec)	$e$ (in/in)
1	0.755	0.683	0.660	0.023	1.017	0.0954
2	0.683	0.607	0.590	0.017	1.158	0.111
3	0.607	0.539	0.524	0.015	1.234	0.112
4	0.539	0.378	0.356	0.022	2.237	0.299
5	0.378	0.255	0.242	0.013	2.802	0.325
6	0.255	0.173	0.148	0.025	3.393	0.322
7	0.173	0.113	0.094	0.019	4.301	0.347
8	0.113	0.070	0.053	0.017	5.611	0.380
					Total Strain	2.378
9	0.070	0.046	0.025	0.021	6.795	0.350
					Total Strain	2.798

### C. MACHINING OF TENSILE COUPONS

Tensile test coupons were machined from all rolling samples to the dimensions of Figure 1. The composite material proved to be very abrasive, and machining the composite coupons required the use of diamond cutting tools.

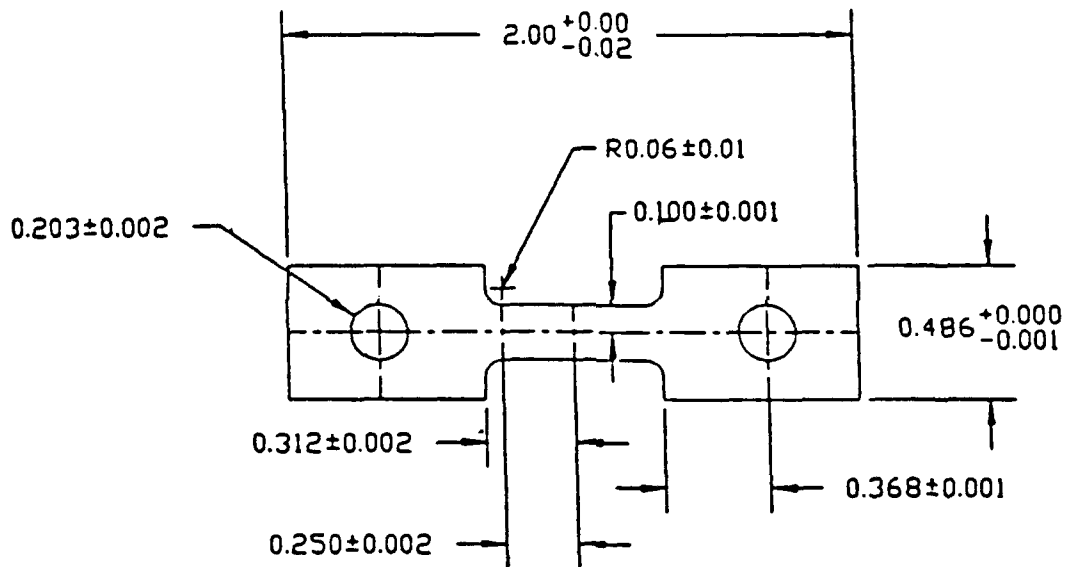


Figure 1. Tensile Test Specimen Drawing

#### **D. TENSILE TESTING**

Tensile test data obtained from the Instron Tension Tester (Model 6027) was processed with a Hewlett Packard Model 3852A Data Acquisition Unit, and a plot of load (KN) versus time (min) was obtained. All tests utilized a constant cross head speed of 0.508 mm/min and were conducted at ambient temperature. Engineering stress versus engineering strain plots were generated from the raw test data by extrapolating the elastic regions slope onto the load versus time curve to determine the range of plastic deformation for the curve. Engineering stress was obtained using a PC based program, calculating engineering stress based on the actual tensile sample cross sectional area.

#### **E. AGING STUDY**

To determine the aging response for the materials, an aging study was conducted using hardness as a preliminary gage of the 'ultimate tensile strength' (UTS). The hardness of the coupons was tested by a Rockwell Hardness Tester (Model Nr 1JR) using schedule "F" (1/16" diameter ball and 60 Kg mass). Based on the Rockwell results, a series of Instron tensile tests was performed using tensile coupons aged to similar peak hardness conditions. The aims of the aging experiment were to determine the aging response of the composite in comparison to the unreinforced matrix material, and to better understand the relationship of the

aging process to varying TMP parameters, thereby identifying the optimum aging condition for the material. The hardness and tensile results are graphically represented in the results section with the summary data tables contained in the appendices.

### **1. SOLUTION TREATMENT**

A portion of sample material was cut from all final rolling passes. The material was immediately quenched to preserve it in its as-rolled state and sectioned into both Rockwell hardness test coupons (dimensions  $\approx 1$ " by 2") and Instron tensile coupons as were discussed in the previous section. All coupons were solution treated at 560c for 90 minutes prior to aging.

### **2. AGING TEMPERATURES**

Aging temperatures were picked on the basis of handbook data and the previous work done by T. A. Schaefer whose aging study was conducted at 160°C. The temperatures used for this work used 160°C as the middle point for temperature selection. The material was aged at 135°C, 150°C, 175°C and 200°C to determine the effect of both lower and higher temperatures on the aging process.

### **3. AGING COMPOSITE VS UNREINFORCED ALUMINUM**

The unreinforced 6061 base aluminum was aged simultaneously under the same conditions to serve as a control group with which to gage the response of the composite material.

## F. OPTICAL MICROSCOPY

Both the composite and the unreinforced 6061 aluminum were examined with the optical microscope (Zeiss ICM-405 Optical Microscope). Pictures were taken with Polaroid, Type T-55 film.

### 1. POLISHING SCHEDULES

The standard polishing techniques, although used successfully for the unreinforced 6061 aluminum, proved to be inadequate for polishing the composite samples. The standard polishing techniques left residual scratches on the surface of the composite; therefore, the following composite polishing schedule was used:

Table 3. COMPOSITE POLISHING SCHEDULE

Step #	Polishing Medium	Time (min)	Wheel RPM	Comments
1	320 Grit	2	180-200	Light pressure
2	400 Grit	2	180-200	Light pressure
3	600 Grit	2	180-200	Light pressure
4	6 Micron diamond paste (metadi)	3	180-200	Light pressure
5	3 Micron diamond paste (metadi)	2	180-200	Light pressure
6	Collodial Silica	remove all scratches	180-200	Light pressure wear gloves

## **G. SCANNING ELECTRON MICROSCOPE (SEM)**

A Cambridge, Stereoscan 200 Scanning electron microscope equipped with a Kevex Super 8005 Composition Analyzer was used to examine the fracture surfaces of the tensile samples, to determine particle sizes and distributions, and analyze the composition of precipitated particles. Fracture surfaces were examined in the SEM mode and the EDX mode was used for particle composition analysis.

## IV. THEORETICAL PRESENTATION

### A. THE EFFECT OF SECONDARY TMP ON MICROSTRUCTURE

The microstructural effects of secondary TMP were assessed primarily by optical microscopy. The effects of the TMP were evaluated by the following microstructural characteristics:

- Precipitation
- Solute content
- Redistribution of reinforcement particles
- Recovery/recrystallization
- Grain size refinement

These microstructural features will have a pronounced influence on the final mechanical behavior of the material.

### B. UNREINFORCED MATRIX

The unreinforced 6061 matrix represents the "...glue to bind" [Ref. 16] the material together. To a first order approximation, the microstructural changes and their influence on the properties of the unreinforced matrix are of prime importance to the final behavior of the composite. This assumption is valid since

the combination of the matrix and the particles provide the characteristics of the composite.

### 1. Al 6061 COMPOSITION

Al 6061 is an age-hardenable Al-Mg-Si alloy with the nominal composition listed below in Table 4.

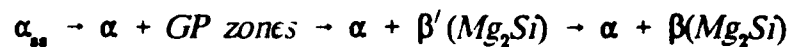
**Table 4. COMPOSITION LIMITS FOR 6061 ALUMINUM IN WEIGHT PERCENT**

Mg	Si	Fe	Cu	Zn	Mn	Ti	Cr	Others
0.8 to 1.2	0.4 to 0.8	0.7 max	0.15 to 0.4	0.25 max	0.15 max	0.15 max	0.04 to 0.35	0.05 max

Although other precipitates such as Si, SiO<sub>2</sub>, Fe, Cr etc. are known to occur in 6061, the dominate precipitate in this alloy is the intermetallic compound Mg<sub>2</sub>Si.

### 2. Mg<sub>2</sub>Si PRECIPITATION

The precipitation of Mg<sub>2</sub>Si may strengthen the matrix aluminum. During low temperature aging, the 6XXX alloy exhibits several coherent precipitates before the final equilibrium phase, β, is produced:



Conventional heat treatment of the 6061 aluminum involves solution treating, quenching and then artificial aging at  $\approx 160^{\circ}\text{C}$  for 18 hours.

[Ref. 17] When aged to peak strength,

the precipitation is terminated with the formation of  $\beta'$ .

The processing temperatures employed in this work ( $350^{\circ}\text{C}$  and  $500^{\circ}\text{C}$ ) are much higher than this conventional aging temperature. During the processing of the 6061, the equilibrium volume fraction of the  $\beta$  ( $\text{Mg}_2\text{Si}$ ) is expected to precipitate. Such precipitation will reduce the amount of Mg and Si in solid solution. If the precipitated  $\text{Mg}_2\text{Si}$  is in the form of large equiaxed particles ( $> 3\mu\text{m}$  diameter) with large interparticle spacing, then the particles may not significantly contribute to the material's strength through the mechanism of Orowan bowing. Yet, such precipitation will reduce the solid solution strengthening effect of the Mg and Si.

The ternary phase diagram of  $\text{Mg}_2\text{Si}$  solubility in 6061, presented in Figure 2, [Ref. 18] shows a decreasing solubility for  $\text{Mg}_2\text{Si}$  with decreasing temperature.

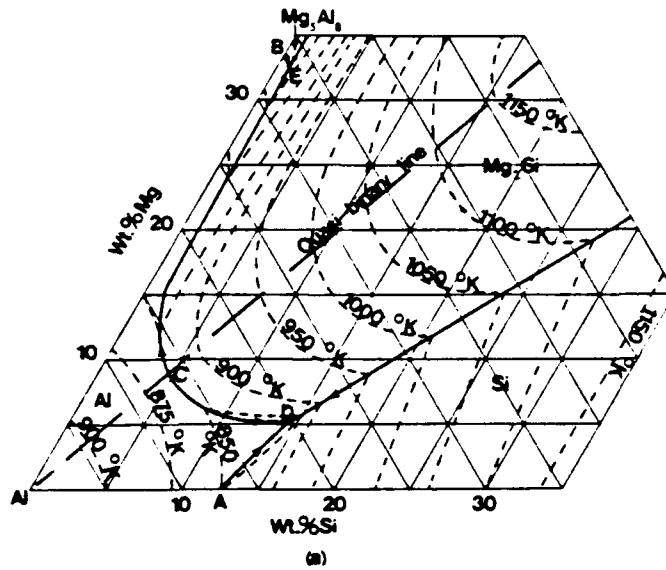


Figure 2. Phase diagram of Al-Mg-Si system showing the solvus line for  $\text{Mg}_2\text{Si}$ . [Ref. 18]

Higher processing temperatures will result in more Mg and Si in solution compared to lower processing temperatures.

### 3. RECOVERY/RECRYSTALLIZATION

Recovery is a lower temperature process which results in a reduction (annihilation) of dislocations and a rearrangement (polygonization) of dislocations into subgrain structure. Residual stresses associated with deformation are slightly reduced due to recovery. Conventional recrystallization is a nucleation and growth process which eliminates dislocations as new grains are formed. The heterogeneous nucleation of these grains requires a critical strain energy content which is reduced in the vicinity of any interface which may serve as a nucleation site. If the interface is a non-deformable particle, then a critical radius is required in order for the particle to serve as a nucleation site (see discussion on PSN). Therefore, it is expected that the presence of the  $Mg_2Si$  may assist recrystallization as well as contribute to the control of later grain growth.

The precipitated  $Mg_2Si$  particles could actually impede subgrain growth needed for initiation of recrystallization. If  $F_v/d > 0.1\mu m^{-1}$ , where  $F_v$  is the volume fraction of particles and  $d$  is the particle diameter, the particles are too closely spaced, and recrystallization can be significantly impeded. [Ref. 19]

#### 4. GRAIN SIZE

The recrystallized grain size is a complex function of the competing influences of temperature/time (activation energy), surface energy considerations, and the presence of additional phases. Higher temperatures cause faster growth and a coarser grain microstructure, and the grain size,  $D$ , is related to the yield strength,  $\sigma_y$ , by the *Hall-Petch* equation:

$$\sigma_y = \sigma_o + KD^{-1/2} \quad (5)$$

Where  $\sigma_o$  and  $K$  are material constants. Decreasing the grain size increases the strength and also the strain hardening rate for the material. The strengthening effect is realized as refinement of the grain size provides more obstacles to dislocation movement as the grain boundaries' high energy areas serve as dislocation blockers. However, the contribution to the volume free energy,  $\Delta F_v$ , associated with the surface area is much higher than for a larger, more coarsened grain structure. This energy differential (gradient) is associated with the inefficient packing of atoms at the grain boundary interfaces, and provides the driving force for grain growth [Ref. 20]. The small grain size is unstable, and a lower overall energy is achieved by grain growth but with an undesirable decrease in ductility and strength. Therefore, the benefits of the grain refinement process have a limit where there is sufficient energy to nucleate new grains and yet, the grain size has not increased significantly.

**a. PSN**

As discussed, the precipitated  $Mg_2Si$  particles may serve as sites of 'particle stimulated nucleation' (PSN) if they are greater than a critical radius for this phenomenon. According to Humphreys [Ref. 21], this critical diameter is  $\approx 1\mu m$  for materials processed at ambient temperature. The conditions for PSN at elevated temperatures have been shown to depend on strain rate, strain and processing temperature [Ref. 22]. However, as previously stated, the lack of  $Mg_2Si$  precipitates above this size in the matrix makes their contribution small. At higher temperatures fewer  $Mg_2Si$  precipitates are expected to be present, and so their effect is expected to be even less of a factor.

**C. COMPOSITE**

Humphreys astutely states that "...the essential difference between particulate aluminum composites and monolithic [unreinforced] alloys is that the volume percentage of large undeformable particles (10-20 volume %) is significantly greater than in conventional alloys (0-2 volume %) [Ref. 23]. For the cast and extruded Al- $Al_2O_3$  composite, the large volume percentage of undeformable  $Al_2O_3$  particles in the softer 6061 matrix significantly contributes to all aspects of microstructural evolution during the TMP.

## 1. EFFECTS DERIVED FROM PARTICLE REDISTRIBUTION

### *a. BENEFITS OF REDISTRIBUTION*

Earlier work done by Lt T. A. Schaefer established the microstructural benefits achieved by extrusion of the 10 volume percent composite over the as-cast condition [Ref. 24]. Schaefer demonstrated that the extrusion performed by the manufacturer (DURALCAN) clearly resulted in a more homogeneous distribution of the ceramic particles which led to increased strength as well as increased ductility. Schaefer also demonstrated that the subsequent rolling continued to redistribute the particles and decreased the effective diameter of the particles as the clusters were broken up.

## 2. PARTICLE MATRIX INTERACTIONS

### *a. PARTICLE DEFORMATION ZONES*

Based on the pioneering work of Ashby [Ref. 25], Porter and Humphreys [Ref. 26], and Humphreys and Kalu [Ref. 27], have noted that the incompatibility between a deforming matrix and non-deformable particles results in dislocations being generated at the particles as they rotate to relieve stresses. Hirsch and Humphreys have observed prismatic loops forming in materials containing small, non-deformable particles at small strains. [Ref. 28] Meyers gives the approximate dislocation density produced as follows: [Ref. 29]

$$\rho_g = \frac{4F_v \gamma}{br} \quad (6)$$

where  $\rho_g$  is the dislocation density,  $F_v$  is the volume fraction of the particles,  $b$  is the burgers vector,  $r$  is particle radius, and  $\gamma$  is the strain. The dislocation density is directly related to the work hardening rate. Figure 3 [Ref. 30] depicts a simplified schematic of this phenomenon.

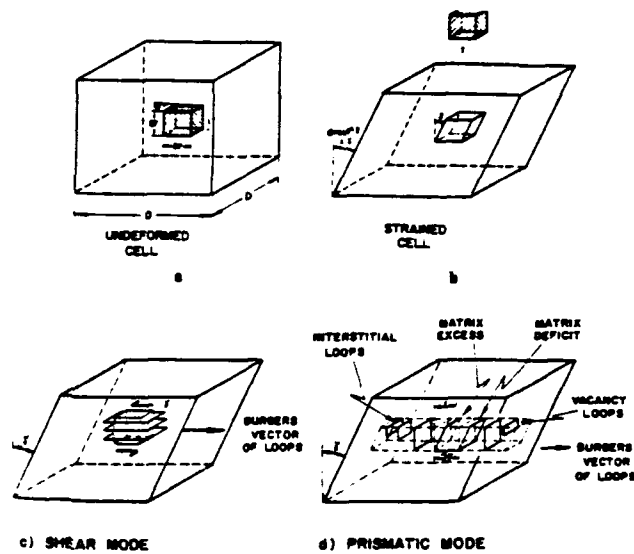


Figure 3. Schematic of formation of the particle's deformation zone.

Essentially, this is a visualization of the accommodation of the non-deformable particle by local plastic strain,  $\gamma$ , of the matrix. Material is removed to reinsert the undeformed particle into the deformed matrix and prismatic dislocation loops may be generated in the process. [Ref. 31]

For particles of the size range encountered in MMC's, plastic relaxation results in a region close to the particle called a deformation zone in which the surrounding matrix becomes rotated with respect to the particle in order to relieve stress. The dislocation configurations depend primarily on the particle size and shape. [Ref. 32] The 10-30% strains during the rolling of material for this work are expected to result in deformation zones in the vicinity of the  $Al_2O_3$  particles.

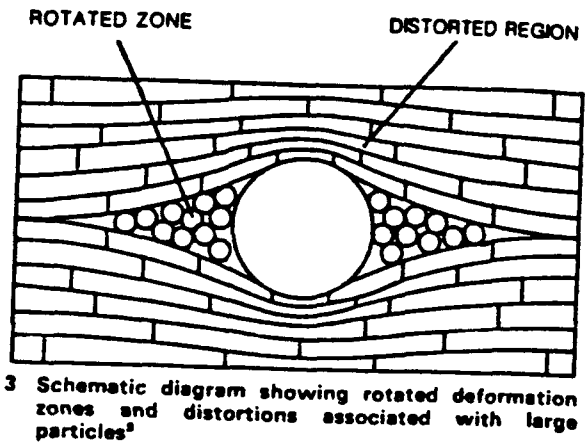


Figure 4. The deformation zone as shown by Humphreys.

The precipitates of  $Mg_2Si$  may also contribute to the development of these deformation zones as shown in Figure 4. [Ref. 33]

However, due to the sheer number of  $Al_2O_3$  particles in

comparison, the  $Mg_2Si$  contribution likely is minimal.

These deformation zones contribute both to the increased strain hardening and the to the early aging response of the composite. Each of these effects will be subsequently discussed.

#### *b. OBSTACLES TO DISLOCATION MOVEMENT*

The deformation zones disturb existing slip patterns and impede the movement of dislocations in the surrounding matrix. The deformation zones extend into the matrix, thereby increasing the overall dislocation density of the composite material. In large volume fraction composites, where the particle spacing approaches the dimension of the particles themselves, this effect can even lead to a weakening of the composite as the adjacent deformation zones interact. [Ref. 34]

### 3. PARTICLES AS SITES FOR NUCLEATION (PSN)

The formation of deformation zones is a prerequisite for PSN. When a deformed material containing deformation zones is annealed, PSN may occur provided that the following conditions are satisfied:

- high dislocation density exists,
- large orientation gradient is present between the particle and matrix. [Ref. 35]

As seen in Figure 5 [Ref. 36], the  $12\mu\text{m}$  diameter  $\text{Al}_2\text{O}_3$  particles is sufficient to stimulate heterogeneous nucleation with a strain (reduction) as low as 20 percent. The contributing effects of PSN nucleation along with particle redistribution contributes to grain refinement in the composite.

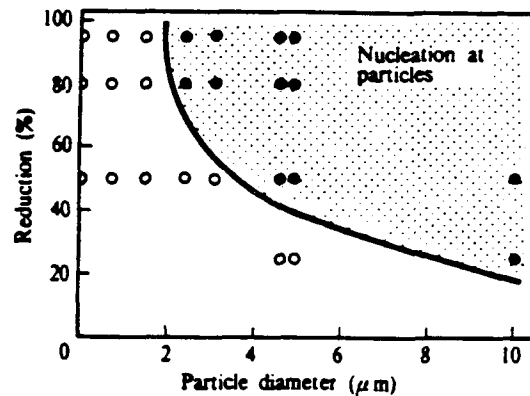


Figure 5. Size vs PSN capability.

#### 4. GRAIN SIZE REFINEMENT

The presence of a second phase in the microstructure helps prevent grain growth and keeps the recrystallized grain size small.[Ref. 37] As seen by Figure 6 [Ref. 38], it is the size of the particles and their volume fraction which determine the final grain size.

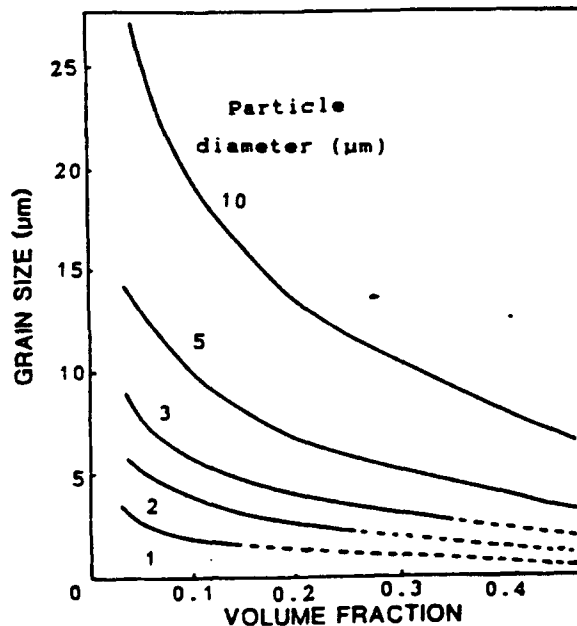


Figure 6. Grain size as a function of volume fraction and particle size.

In the composite, the grain size is approximately proportional to particle spacing for PSN conditions, and the diameter of the grain is patterned by the following model:[Ref. 39]

$$D_n = d / F_v^{1/3} \quad (7)$$

where  $d$  is the particle diameter and  $F_v$  is the volume fraction of the particles.

Therefore, the presence of  $Al_2O_3$  particles embedded in the matrix would be expected to produce smaller grains than the unreinforced matrix under similar processing.

The effect of grain refinement on the ambient temperature strength is generally assumed to follow the Hall-Petch theory in which grain size relates directly to the strength:

$$\sigma_y = \sigma_o + kD^{-1/2} \quad (8)$$

The value of the grain size exponent ( $1/2$  in this theory) has been questioned by Cottrell, et al.; however, the veracity of the general strengthening effect due to decreasing grain size is accepted. The grain size reduction associated with the particles as sites for PSN, may also increase the ductility by enhancing the strain hardening rate of the composite.

## 5. AGING IN THE COMPOSITE

The aging process is accelerated in the composite as a result of the deformation in the vicinity of the  $Al_2O_3$  particles. The dislocations in the deformation zones assist the formation of GP zones by providing heterogeneous nucleation sites for these zones.

## V. RESULTS AND DISCUSSION

### A. EFFECT OF PROCESSING ON MICROSTRUCTURE

The role of the processing on microstructure is the primary focus of the results and discussion section. The processing effect is the primary determinant of the material's final microstructure and thereby its mechanical behavior. The effect of processing of the composite may be viewed as the sum effect of processing of the unreinforced matrix, and the interaction between the matrix and the reinforcement particles. Effort was made to distinguish the effects of processing on the unreinforced aluminum from those on the Al-Al<sub>2</sub>O<sub>3</sub> composite by similarly processing unreinforced matrix aluminum along with the Al-Al<sub>2</sub>O<sub>3</sub> composite. The unreinforced aluminum served as a control group for analyzing combined effect due to processing.

The processing parameters analyzed were total strain, processing temperature, annealing times and, finally, aging heat treatment. The microstructural effects of interest were the precipitation of particles and resulting equilibrium solute content, particle size and spacing, and recrystallization and the relative grain size refinement in both materials. The microstructure was assessed by both optical and scanning electron microscopy and, implicitly, by the mechanical behavior of the material. A

first attempt at optimization of the composite's processing was performed to achieve beneficial composite properties based on the results of earlier work.

Since the unreinforced matrix is the primary load bearing constituent in a particulate MMC, the effects of processing on its microstructure and resulting mechanical behavior are of crucial importance. The effect of processing of the unreinforced matrix is addressed separately to provide insight into the matrix contribution to the composite.

## **1. PROCESSING EFFECTS ON UNREINFORCED MATRIX**

The processing of the unreinforced matrix led to a general strengthening of the matrix coupled with a loss of ductility. The warm rolling of the material to a total rolling strain of approximately 2.9 significantly increased the dislocation density due to work hardening by the rolling strain. The as-processed behavior is explained in several ways.

### ***a. INCREASE IN DISLOCATION DENSITY***

Working the material increases the number of dislocations present. The material, being rapidly quenched at the exit of the final rolling pass, exhibits the usual behavior associated with a worked metal with the increase in strength accompanied by limited ductility.

## ***b. PRECIPITATION OF PARTICLES***

Examination of the as-processed material processed at 350°C revealed the presence of particles. Subsequent EDX analysis of several of the particles showed their composition to be Mg<sub>2</sub>Si, SiO<sub>2</sub>, and intermetallic compounds containing Cr, Fe and Ni. As expected by the phase diagram, the Mg<sub>2</sub>Si was observed in the greatest abundance. The particles ranged from <1μm to 10μm as seen in Figures 7 through 10. They are generally much larger than the 100-2500 angstroms required to provide dispersion strengthening [Ref. 40]. Therefore, the strength contribution of the particles is expected to be relatively minor due to their large size, low volume fraction and spacing which is expected to be too great to provide effective Orowan bowing. Further research is needed to determine their role in strengthening or in grain refinement. However, the presence of these relatively large precipitates may serve as sites for PSN.

In addition, back scattered SEM micrographs show the presence of other particles of varying sizes as also seen in Figure 7. Some of these particles may contribute to additional strengthening; however, further research is needed to determine their role in the final properties of the material.

**Micrographs of the Unreinforced Aluminum Processed at 350°C**

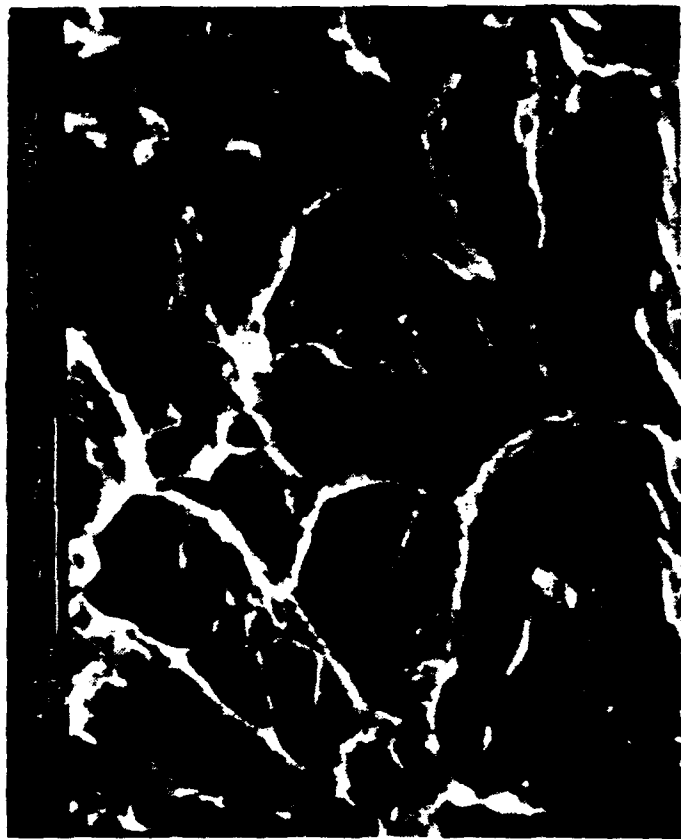


**Figure 9. Presence of intermetallic particles shown in unreinforced aluminum processed at 350°C.**

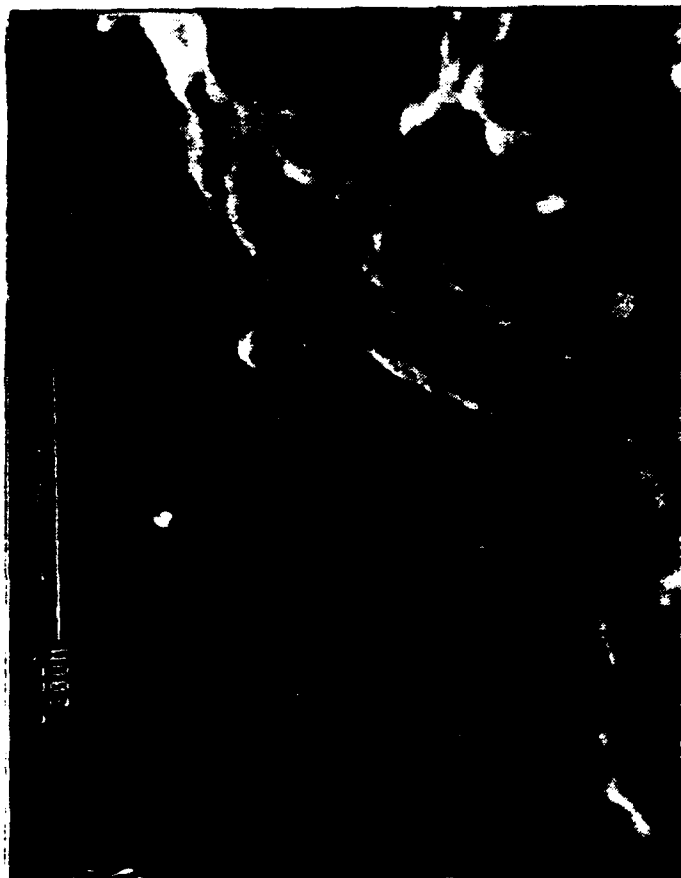


**Figure 10. Particles of MgO shown in unreinforced aluminum processed at 350°C.**

**Micrographs of the Unreinforced Aluminum Processed at 350°C**

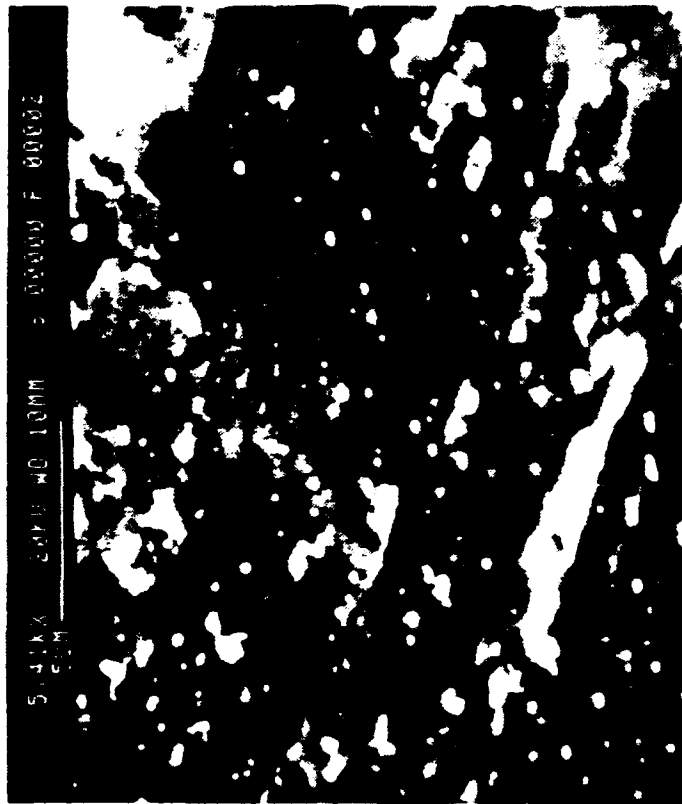


**Figure 7. SEM micrograph showing the presence of particles of varying size in unreinforced aluminum.**



**Figure 8. Particles of SiO<sub>2</sub> shown for unreinforced aluminum processed at 350°C.**

### *c SOLUTION STRENGTHENING OF Mg AND Si*

The presence of relatively coarse  $Mg_2Si$  particles results from the high processing temperatures involved in this work. The elevated processing temperatures result in the precipitation and coarsening of equilibrium  $\beta$  ( $Mg_2Si$ ), and the material being in the overaged condition. The amount of  $Mg_2Si$  precipitation is an indicator of the content of Mg and Si remaining in solution. Since both Mg and Si are effective solid solution strengthening constituents in the alloy, the presence of the coarse  $Mg_2Si$  particles serve not to strengthen, but more as a depository of Mg and Si from solution. The phase diagram of the quasi-binary solubility line for  $Mg_2Si$  increases with increasing temperature and the solute content of the Mg and Si is shown to decrease with a higher processing temperature. Plotting the stress versus strain curves of the unreinforced aluminum processed at both temperatures shows a higher UTS for the material processed at 500°C. This increased strength is consistent with a large strength contribution due to the Mg and Si content of the solid solution.

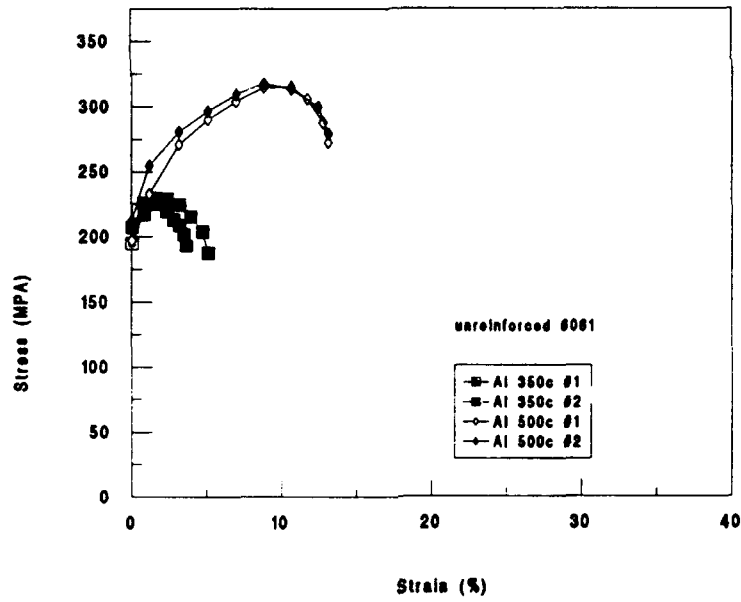


Figure 11. Stress vs strain curves for unreinforced aluminum processed at 350°C and 500°C.

Table 5. COMPARISON OF STRENGTHS VS. TEMPERATURES FOR UNREINFORCED ALUMINUM

Processing Temperature (°C)	Yield Strength (MPA)	UTS (MPA)
350	205	225
500	205	280

#### *d. GRAIN SIZE REFINEMENT*

(1) Sites for PSN of Recrystallization. The precipitates present in the unreinforced aluminum are of sufficient size to serve as sites for PSN of recrystallization the processing conditions experienced in this work [Ref. 41]. However, the volume fraction is such that any contribution made by their presence is likely to be low. This may be shown by the model for grain size refinement resulting from PSN of one grain per site where the grain size becomes inversely related to the volume fraction of particles.

$$D_n = \frac{d}{F_v^{1/3}}$$

where  $D_n$  is the grain size resulting from the PSN.

(2) Particle Pinning. Experiments have shown that when particles are closely spaced subgrain growth and coalescence necessary for recrystallization nucleation is impeded. The material will recover but may not recrystallize [Ref. 42]. If  $F_v/d > 0.1 \mu\text{m}^{-1}$  the recrystallization may be impeded [Ref. 43] and the grain size of the initial material reduced. Again, SEM examination revealed a low volume fraction for the precipitated particles in the unreinforced material which suggests that these particles have little influence in refining the grain size.

## 2. PROCESSING EFFECTS ON THE COMPOSITE

The effect on the matrix gives insight into the effects anticipated for the composite. As mentioned, the presence of the low volume fraction of  $Mg_2Si$  particles in the unreinforced matrix contributes little to the final properties of the material aside from absorbing solute. The strengthening and loss of ductility of the unreinforced matrix is shown to be predominately a result of the work hardening associated with rolling strain. The effect of the composite is complicated by the large volume fraction of non-deformable  $Al_2O_3$  particles not present in the unreinforced matrix. This abundance of  $Al_2O_3$  is expected to provide sites for repeated PSN during the successive rolling passes and annealing to a very fine grain size.

### a. PARTICLE REDISTRIBUTION

As previously discussed, the work of Schaefer showed that extrusion of the cast composite resulted in a better dispersion of the particles and an increase in ductility and yield strength when compared to the as-cast condition. As will be shown, further

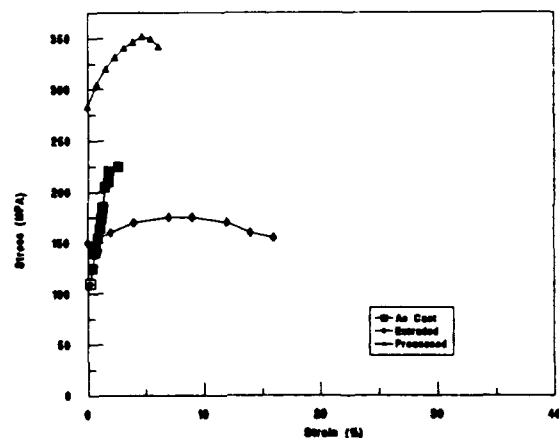


Figure 11. Comparison of the stress vs strain behavior of as-cast, extruded and as-processed composite ( $550^{\circ}C$ ).

processing continues to distribute the particles throughout the matrix. This result of this effect is seen in Figure 12.

The as-processed composite is also included on the graph and shows a continuation of the strengthening with further processing but with a loss of ductility. As previously seen, the unreinforced aluminum matrix in a similar as-processed condition showed increased strength and decreased ductility due to strain hardening. Comparing the strengths of the composite and unreinforced aluminum matrix shows additional strengthening due to the presence of the particles. Subsequent sections will explore and attempt to separate the effect of the particles from the effects of processing on the matrix itself.

(1) *As-Received Material.* The as-received composite material used for this work was cast and then subsequently hot extruded. Previous optical microscopy done by Schaefer demonstrated the homogenization of particles with extrusion. The as-received, extruded material showed some clustered regions and banding in the direction of extrusion. The effective particle diameter of the as-received material was a function of the cluster size [Ref. 44].

(2) *Effect of TMP.* Optical micrographs of the as-rolled material taken after each of several rolling passes showed a redistribution of the  $Al_2O_3$  particles which became more homogeneous with processing. This is clearly seen when comparing Figures 13 through 16. The particles became increasingly

dispersed and more homogeneously distributed throughout the material as a result of the strain of rolling. This result is consistent with previous studies by Schaefer and Schauder [Ref. 45].

Composite Micrographs for 500°C Processing Temperature



Figure 15. Roll #3 ( $\epsilon=0.347$ ) showing clusters and banding.



Figure 16. Final roll ( $\epsilon=2.80$ ) showing more homogeneous distribution of particles.

Composite Micrographs for 350°C Processing Temperature



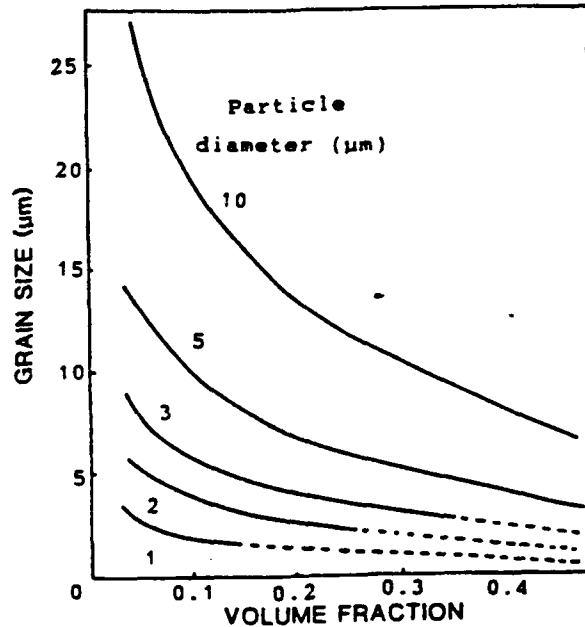
Figure 13. Roll #3 ( $\epsilon=0.337$ ) showing clusters and banding.



Figure 14. Final roll ( $\epsilon=2.798$ ) showing more homogeneous particle distribution.

**b. PSN SITES**

As the original clusters were broken up, the effective particle diameter was progressively reduced, and concurrently, the number of possible PSN site was greatly increased. Optical microscopy showed the diameter of individual particles to be  $\approx 12 \mu\text{m}$  which was still sufficient to serve as sites for PSN. The high volume fraction of the



individual particles provides numerous sites for PSN of recrystallization and

Figure 17. Grain size predicted on the basis of particle stimulated nucleation of recrystallization.

may lead to fine grains as shown in Figure 17. [Ref. 46] Actual recrystallization of nucleation and accompanying grain refinement was shown to occur in this material by Macri. [Ref. 47] He demonstrated refinement of grain size as a result of the processing of the composite. This PSN of recrystallization is enabled both in the intermediate anneals between rolling passes and in the post-roll stabilization. It results in the formation of new, smaller grains, and the size of the new grains help determine the final strength of the material by

the *Hall-Petch* relationship. The relative effects of the  $\text{Al}_2\text{O}_3$  particles are far greater in comparison to the particles that precipitate in the unreinforced aluminum will be addressed.

(1) **Particle Size and Volume Fraction Effects.** The  $\text{Al}_2\text{O}_3$  particles are roughly twice as large as the precipitated particles observed in the unreinforced aluminum, and their volume fraction is many times greater. As seen in Figure 17, the grain size resulting from particle stimulated nucleation of recrystallization is a result of both the individual particle size and the volume fraction. From Figure 17, the large volume fraction of  $\text{Al}_2\text{O}_3$  can compensate for the size difference may still achieve refined grain size.

In the as-processed condition, there is a secondary effect of the reinforcement by particle pinning. Prior to recrystallization, there is increased dislocation density still present in the material as a result of the strain of processing. In this condition, the particles serve as obstacles to dislocation motion and impede the slip systems inherent to the material structure. This effect is seen when comparing the as-processed strength of the composite to the unreinforced aluminum processed under similar condition that follows.

## B. TENSILE TEST RESULTS

### 1. AS-ROLLED STRENGTH COMPARISON

In previous sections, the microstructural characteristics important to strength were considered. The strength of the material can be hypothesized as the summation of many contributing effect as follows:

$$\tau_{total} = \tau_p + \tau_{\perp} + \tau_{solute} + \tau_{ppt} + \tau_{grainsize} \quad (10)$$

where the contributing effects of particles ( $\tau_p$ ), dislocations ( $\tau_{\perp}$ ), solute content ( $\tau_{solute}$ ), precipitation ( $\tau_{ppt}$ ), and grain size ( $\tau_{grain\ size}$ ), respectively, are expressed as contributors to the total strength ( $\tau_{total}$ ) of the material. Of the effects mentioned, the solute content, grain size and dislocation density are of the most importance in this work. While a direct grain size comparison of the composite to the unreinforced aluminum is not available, the composite is expected to result in a finer grain size due to the extent of ability to produce PSN. To analyze the different microstructures effects associated with the reinforcement particles, the strength of the composite material is compared to the corresponding unreinforced aluminum material processed by the same TMP schedule. This direct comparison must be tempered by the fact that the 6061 used in the comparison is "off the shelf" and not from the same batch as used by the manufacturer of the composite. However, it

shows the increased strength of the composite with the presence of  $Al_2O_3$  particles to the matrix containing only a low volume fraction of precipitated particles.

(1) *350°C Processing Temperature.* Instron tensile test results show

that in the as-rolled condition, the composite was actually more ductile and weaker (both yield and UTS) than the unreinforced 6061 matrix processed by similar TMP treatment. This was a very unexpected result as the composite

was expected to be significantly stronger than the unreinforced matrix in the as-rolled condition. The strength

of the as-rolled 350°C composite is weaker than reported by Schaefer [Ref. 48] but is consistent with the work of Schauder [Ref. 49]. SEM examination of the composite fracture surface revealed 'microvoid coalescence' (MVC) associated with the particles in the composite. Characteristic parabolic depressions appeared on the fracture surface [Ref. 50]. These depressions may reflect weakening of the particle-matrix interface during processing.

The strength of the unreinforced aluminum is consistent with Schaefer's findings. As previously stated, SEM examination of the unreinforced

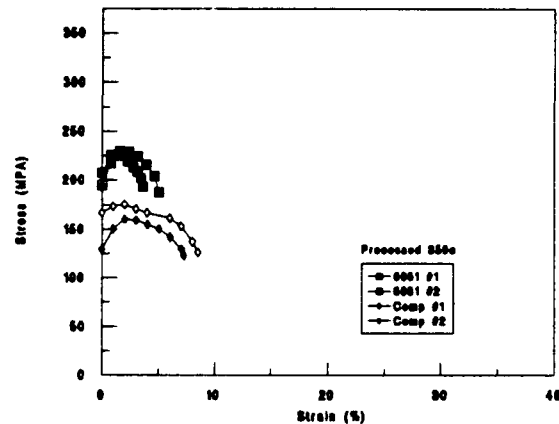


Figure 17. Comparison of the as-rolled strengths of the alumina composite and the unreinforced aluminum

aluminum revealed equiaxed particles of roughly 5 to 10  $\mu\text{m}$  as well as the presence of smaller particles. The contribution of these particles to the unexpected strength of the 350° C is a subject for further research. The most probable explanation for their presence is the impurity content of this particular material.

SEM Photographs of the Fracture Surfaces for 350°C

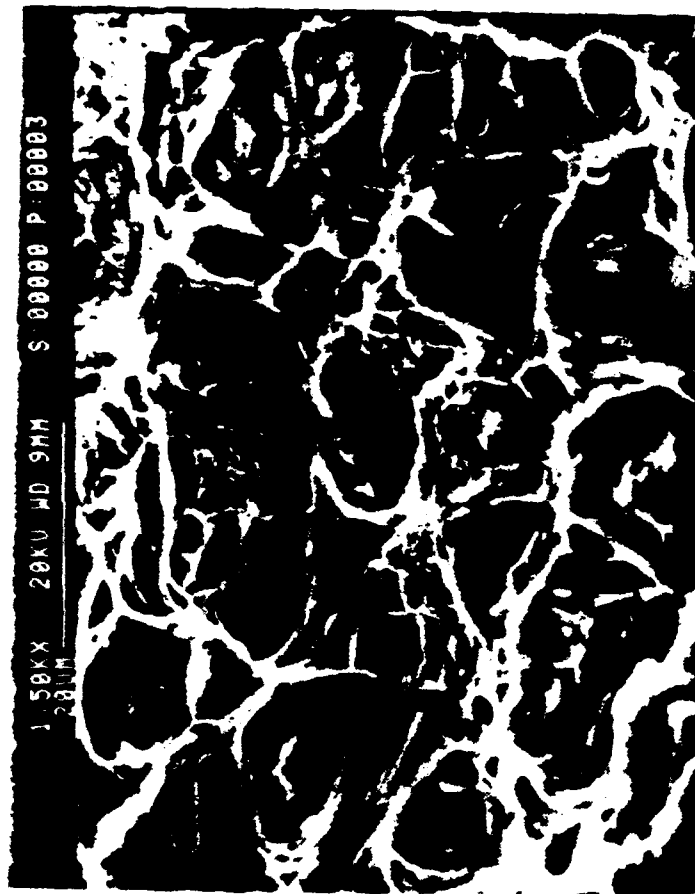


Figure 19. SEM photograph showing microvoid coalescence.

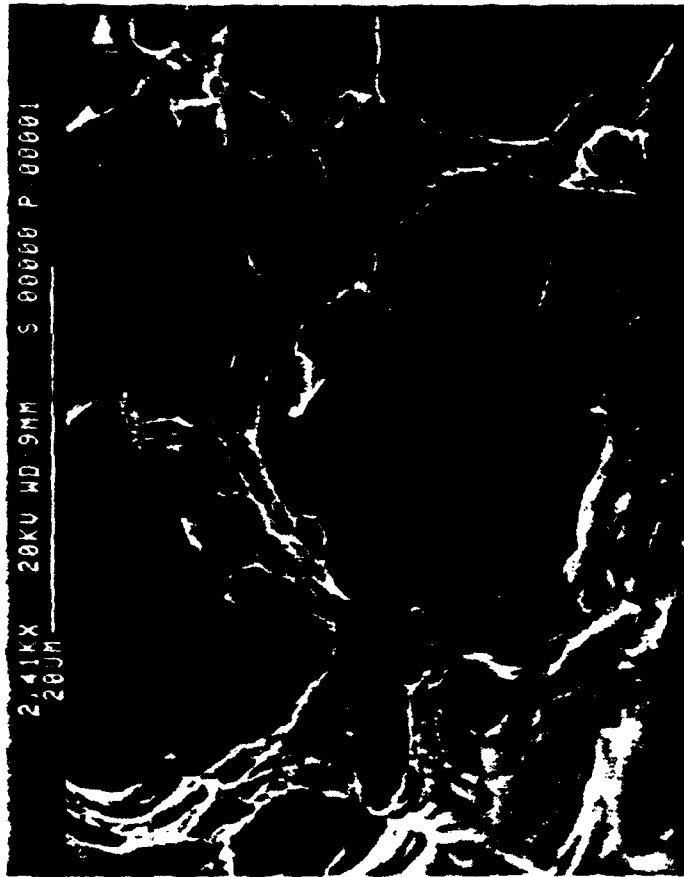


Figure 20. Close up view of a typical void in the Al<sub>2</sub>O<sub>3</sub> composite.

(2) *500°C Processing Temperature.* The 500°C processed material

displays behavior more characteristic of that anticipated for a composite, being both stronger and less ductile than the corresponding unreinforced aluminum. This characteristic behavior is attributed to the effect of the reinforcement particles. In the as-processed condition, the high dislocation density and the interaction of the particles' deformation

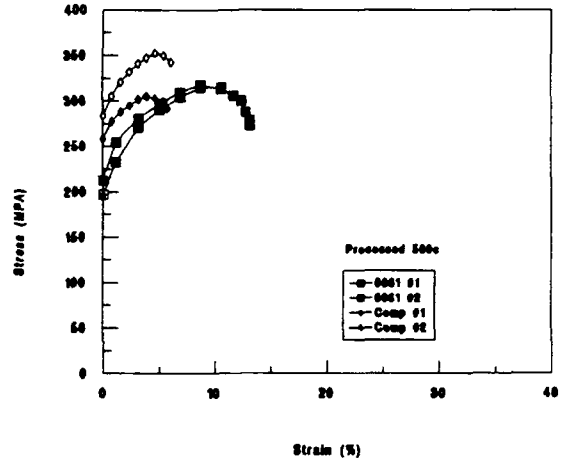


Figure 21. Comparison of the as-rolled strengths of the alumina composite and the unreinforced aluminum

zones with dislocations can act to impede dislocation movement and slip systems. Furthermore, the deformation zones can increase the dislocation density by serving as dislocation sources. The presence of the particles are expected to ultimately result in a finer grain size as they serve as sites for PSN during the intermediate annealing recrystallization.

SEM inspection of the unreinforced aluminum processed at 500°C did not reveal the prevalence of large impurity particles as found in the 350°C material. Also, the precipitation of  $Mg_2Si$  particles contributes little to strengthening as the greater strength and work hardening rate of the composite demonstrate.

## 2. PROCESSING TEMPERATURE EFFECT

The as-rolled strengths of the composite and unreinforced matrix processed at 500°C showed increased strength when compared to the material processed at 350°C. As previously discussed, the effect of temperature on the unreinforced aluminum is directly related to amount of solution strengthening available from the Mg and Si solute and the precipitated particles themselves are expected to provide little in the way of strengthening either by Orowan bowing or as obstacles to dislocation movement or slip. The amount and coarseness of the precipitated  $Mg_2Si$  is related directly to temperature. A greater percentage of solute in solution for the 500°C processed material may account for its greater UTS. At yield, the effect of the solute is not yet an important factor; however, with increasing plastic deformation, the strengthening effect of the solute becomes increasingly pronounced through increased strain hardening rates.

The composite material processed at 500°C is ≈85% stronger and slightly less ductile than the corresponding composite processed at 350°C. The increased strength is a product of the greater solute content at the higher temperature and the lessened ductility is indicative of a greater residual dislocation density. The increased yield strength for the higher processing temperature also may be a result of the increased dislocations formed in the post-roll quenching by differential temperature expansion coefficients at the particle/matrix interface.

This greater strengthening for the as-rolled condition at a processing temperature of 500°C is in conflict with the earlier study performed by Schaefer [Ref. 51]; however, the results are confirmed by other research sources [Ref. 52]. Also, the relationship of the mechanical behavior of the composite vis-a-vis the matrix material is consistent with earlier findings.

**Comparison of Composite and Aluminum Strengths for Both Processing Temperatures**

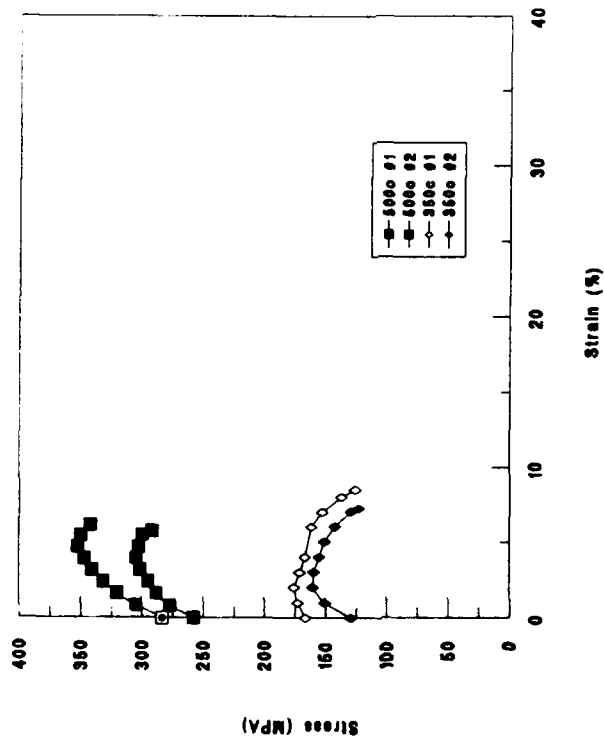


**Figure 22. Comparison of composite strengths for both processing temperatures.**

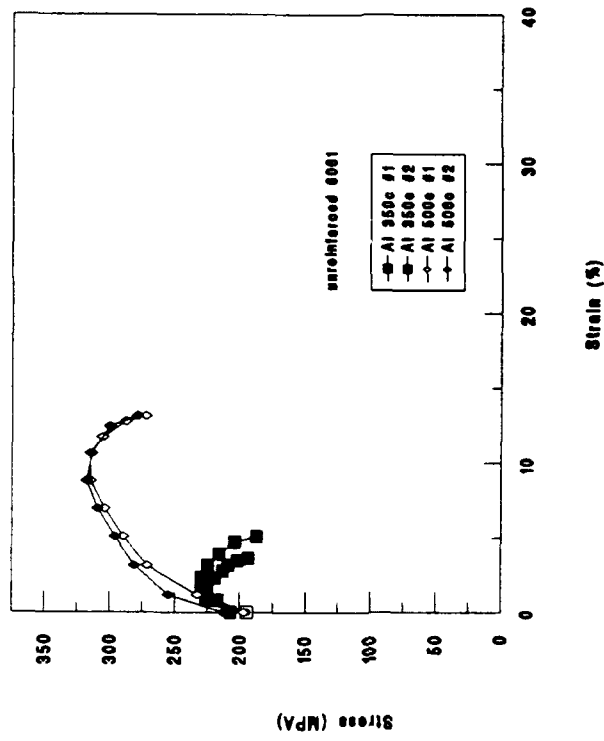


**Figure 23. Comparison of as-rolled 6061 strength at both 350°C and 500°C.**

### 3. STABILIZATION AND DUCTILITY

Stabilization is a post-processing annealing, recrystallization treatment performed at the processing temperature for 30 minutes duration. During stabilization, recrystallization occurs. As seen in the graphical comparison of Figures 24 through 27, stabilization after processing has a profound effects on ductility. Strength is decreased as the material is annealed. The net result of the stabilization is that, at its conclusion, the mechanical behavior between the composite approaches that of the unreinforced matrix. The ductilities of the stabilized composite are roughly equivalent to those of the unreinforced matrix as little or no effect of the previous strain hardening due to processing remain. Most significant is the three-fold increase in the ductility of the composite material.

Again, the processing temperature plays a role. The material processed and stabilized at 350°C may not be completely annealed and maintained a strength advantage in UTS once plastic deformation occurred. For the 500°C processing temperature, the stabilized response of the matrix alloy and the composite are essentially the same in strength and ductility, and all effects of the particles and their associated strain fields have been greatly reduced. The increased ductility of the composite is a significant result, and has significant commercial implications.

10% Volume Aluminum Alumina

Unreinforced Al 6061

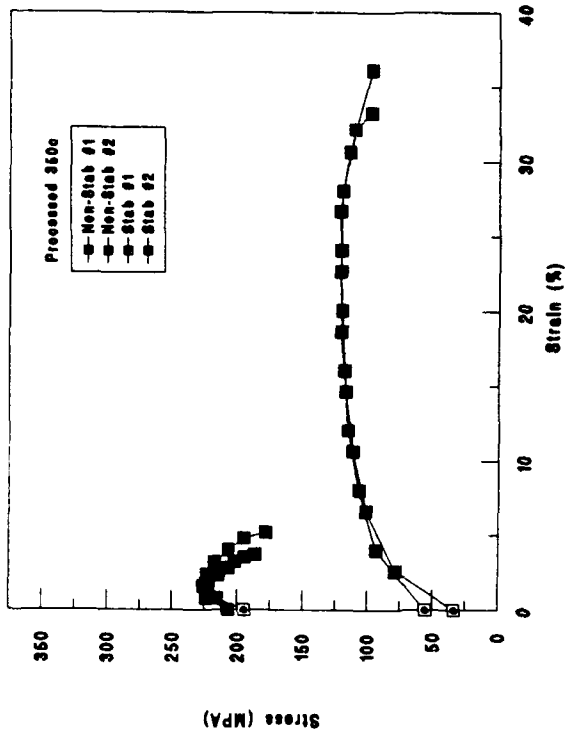
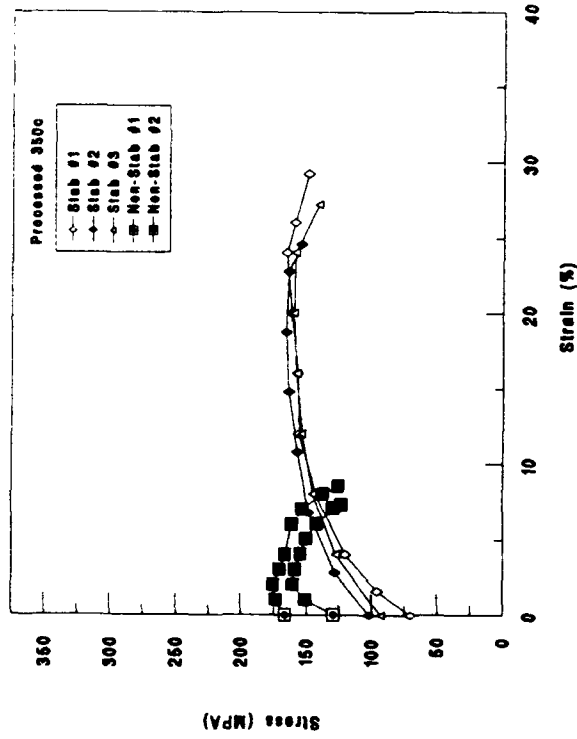


Figure 24. Effect of stabilization on the ductility of composite processed at 350°C

Figure 25. Effect of stabilization on the ductility of unreinforced aluminum processed at 350°C

10% Volume Aluminum Alumina

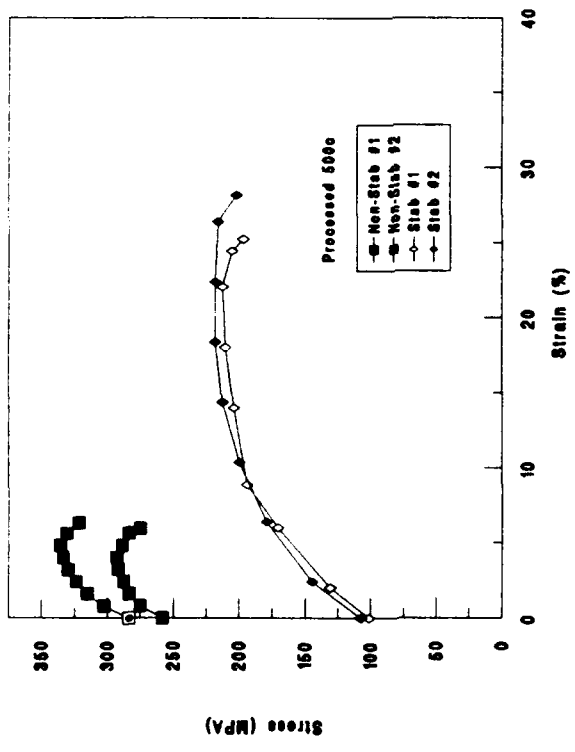


Figure 26. Effect of stabilization on the ductility of composite processed at 500°C

Unreinforced Al 6061

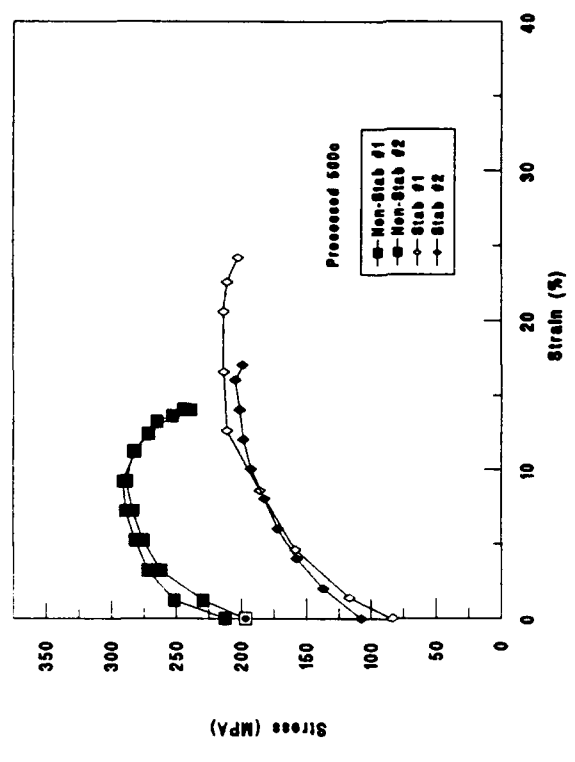


Figure 27. Effect of stabilization on the ductility of unreinforced aluminum processed at 500°C

The improved ductilities of the composite in the annealed condition make the material respond almost as if the discontinuous particles were not present, yet it is fully expected that the characteristic increased modulus, wear resistance and fracture toughness associated with composite materials would be preserved. Also, if the desired strengthening properties of the reinforcement particles could be re-established after the ductility advantages have been exploited, this would be of significant commercial value making composites much more workable.

#### 4. SOLUTION TREATMENT

The effect of solution treatment prior to processing was explored to determine if it altered the end result. One set of samples was solution treated and a second set were not solution treated and each given similar processing regimes. First, small coupons of the sample metal were tested using a Rockwell hardness tester

and showed similar aging response to the solution treated coupons.

Secondly, tensile tests were performed on solution treated and non-solution treated tensile specimens and the plots revealed that there was little or no

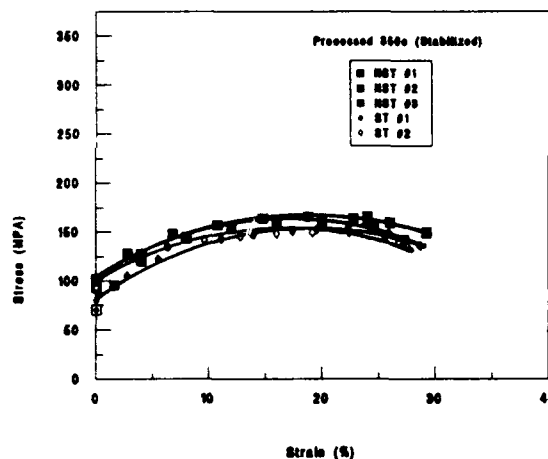


Figure 28. Comparison of solution and non-solution treated tensile tests

difference in the mechanical response of the material based on the solution treatment. The conclusion is that pre-rolling solution treatments are not significant to the final properties of the material.

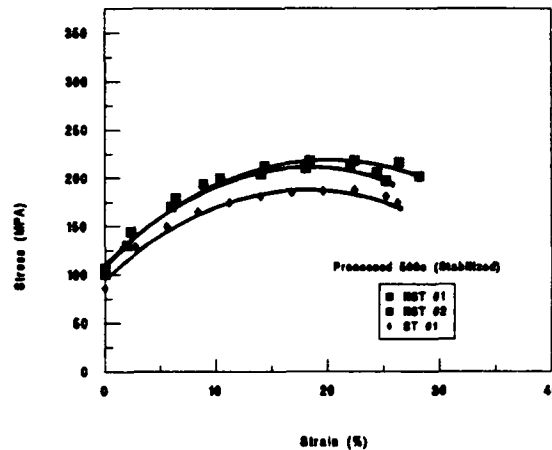


Figure 29. Comparison of solution and non-solution treated tensile tests (500°c)

### C. TOTAL STRAIN

Rolling strains greater than approximately 2.4 were found to be sufficient to produce satisfactory particle distribution to result in a fine grain structure. Samples from rolling passes #8 and #9, corresponding to total rolling strains of 2.37 and 2.80 respectively, showed no significant difference in mechanical properties during tensile tests. Optical microscopy of both samples showed no significant difference in particle distribution.

### D. AGING STUDY

#### 1. HARDNESS TESTING

The composite and unreinforced materials were aged using standard aging heat treatments consisting of a post-rolling quench, solution treatment at 560° C for 90 minutes and aged at a range of temperatures from 150° C to 200° C. Comparison

of the hardness vs time response of the composite versus the unreinforced aluminum shows a general trend for the composite to age faster and to a greater hardness. Figure 30 shows an example of this trend. The complete set of graphs for all temperatures is compiled

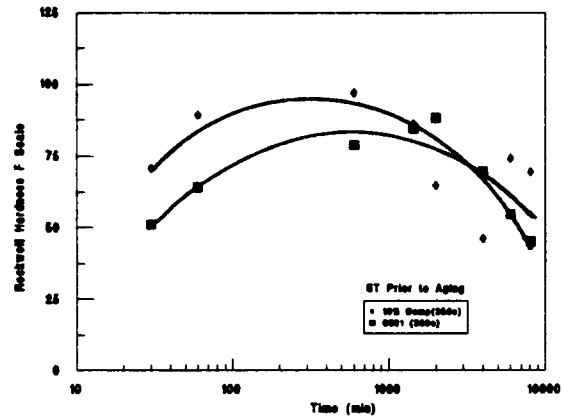


Figure 30. Hardness response for 135°C.

in the appendix. The optimum hardness was achieved between 150°C and 175°C which agrees with handbook data and the earlier work by Shaefer.

## 2. AGED MATERIAL STRENGTH

Based on the hardness results, tensile tests of the materials were conducted on both 175°C and 160°C aged samples to determine the yield stress, UTS, and the strain for the aging process. As before, a representative portion of the results are shown for the material processed at 500°C with the remainder contained in the appendix section.

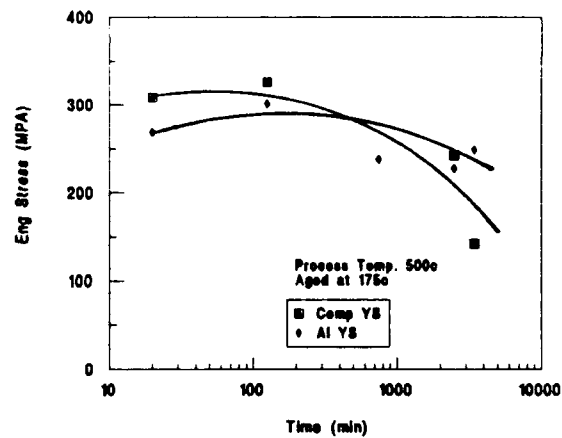


Figure 31. Yield stress vs. time for 175°C aging temperature.

The yield stress that results for aging shows the same trend where the composite results in a greater peak yield stress and an accelerated aging period. As shown in Figure 31, the composite's yield stress of 310 MPA occurring at  $\approx 200$  minutes is roughly 10% greater than the peak unreinforced aluminum, and the period to peak stress is smaller. The composite overages in a shorter period as the thermally produced deformation zones from the post solution treat quench influence the aging process. These regions of high strain energy assist the aging process and accelerate the formation of GP zones,  $\beta'$  and  $\beta$ .

As shown in Figure 32, the increase in UTS is only slightly greater than for the unreinforced peak strength, and the period to attain peak UTS is accelerated. The UTS difference is more pronounced in the  $350^\circ\text{C}$  processed material (see appendix).

Again, the UTS increase in the composite should be a result of the increased dislocation associated with the particle deformation zones for the solute content should be roughly equivalent in both the unreinforced aluminum and composite.

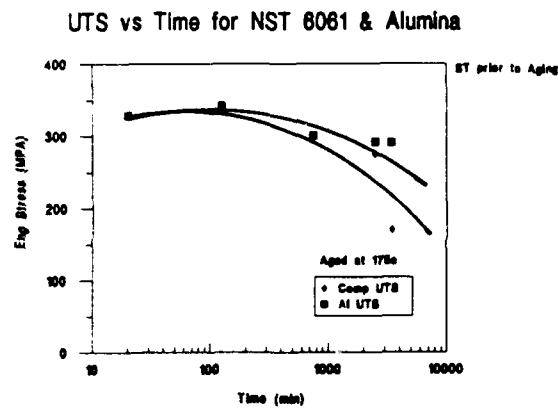


Figure 32. UTS vs. time for  $175^\circ\text{C}$  aging temperature.

The strain of both materials decreases with increasing strength. This reduced strain with increased strength shows the effect of the aging particles and their role as impediments to dislocations motion. The composite shows the combined effect of dislocation zones and aging precipitation as it loses its ductility more quickly.

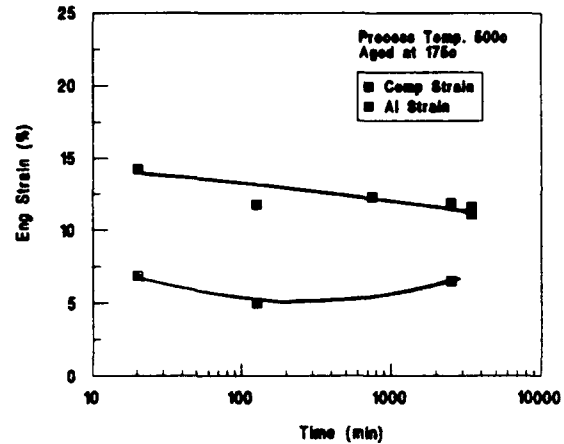


Figure 33. Strain vs time for 175°C aging temperature.

The effect of particles in the aging process may be as a source of dislocations, as a block to dislocation motion, and as an influence to assist in the aging precipitation process.

## E. OPTIMIZATION

Three aspects of TMP are established by the results of this thesis. First, a post-roll stabilization was shown to significantly increase the ductility of the composite material as a result of grain refinement. Secondly, aging was shown to significantly improve the hardness and strength of the composite material although with a loss of ductility. Lastly, the material that was processed at 500°C showed greater strength with comparable ductilities to the material processed at the lower temperature due to the increased solute content. Therefore, in an attempt to

optimize mechanical properties by selective TMP, a group of tensile coupons was processed at 500°C, stabilized, and then aged at 160°C to peak strength. The results of the tensile tests show an improvement over the T6 aging a 6061 aluminum in UTS with slightly less ductility.

The stabilization was utilized versus a full solution treatment to retain a finer grain size. The higher temperature was used to maximize the amount of solute in solution for its precipitation strengthening effect. The

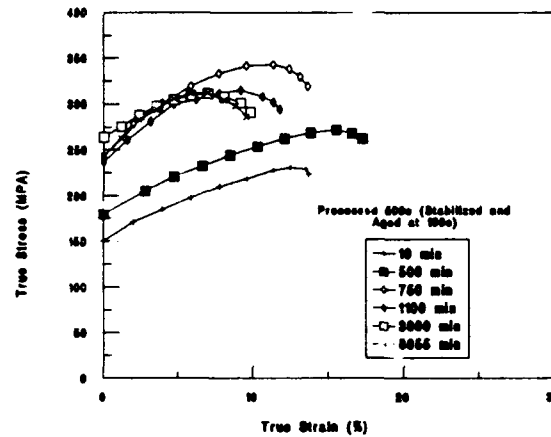


Figure 34. Optimized processing for varying aging times.

gauge of success of these results is best seen when comparing the handbook

values for a T6 aged 6061 aluminum [Ref. 53] to the material above. The ductility produced for the composite is 14% at peak strength which exceeds that of the matrix. This condition refutes the common opinion of composites as being brittle. This ductile condition is achieved with acceptable ductility and suggests that composites processed in this manner can be acceptable replacements in application normally reserved for material of greater ductility. The inherent benefits of composite materials such as increased modulus, thermal resistance, etc can be achieved while having good formability behavior.

**Table 6. STRENGTH AND DUCTILITY COMPARISONS FOR AGED UNREINFORCED 6061 TO STABILIZED THEN AGED COMPOSITE**

Material	Time (hr)	Yield Strength (MPA)	UTS (MPA)	Percent Elongation (%)
Unreinforced 6061 Aged T6	18	276	310	17.2
Stabilized and Aged Composite	8.3	205	263	17
Stabilized and Aged Composite	12.5	278	343	14

The composite material can be processed to be as ductile but 15% weaker (UTS) than the unreinforced aluminum, or it can be processed to be 17% less ductile and 11% stronger. These results show that if selectively processed, the composite can have comparable mechanical response to the unreinforced matrix and still maintain the inherent advantages of being abrasive resistant and possessing an increased modulus for stiffness.

## VI. CONCLUSIONS

1. Processing the composite continually redistributes the particles throughout the unreinforced matrix, achieving a more homogeneous distribution of particles. If PSN is achieved, these particles can serve to refine grain structure thereby enhancing ductility and strength.
2. If selectively processed, the ductility of the composite can be greatly enhanced as a result of recrystallization at the particle PSN sites.
3. Solution treatment prior to processing does not significantly alter the mechanical behavior of the material.
4. A total rolling strain of approximately 2.4 is sufficient to satisfactorily disperse the particles. Further processing does not significantly alter the final mechanical properties.
5. The aging response for the composite showed accelerated aging to a higher peak strength.
6. Optimizing the mechanical properties of the composite can achieve enhanced peak strength and still have a ductility of 14 %. Also, ductilities equivalent to unreinforced aluminum aged to peak strength can be achieved by the composite with a slight loss in strength.

## **APPENDICES**

### **APPENDIX A** **ROLLING SCHEDULES**

**Table 7. 350°C PROCESSED ALUMINA COMPOSITE**

Roll #	T <sub>o</sub> (in)	T <sub>f</sub> (in)	Mill Gap Setting (in)	Mill Deflect. (in)	$\dot{\epsilon}$ (1/sec)	e (in/in)
1	0.755	0.683	0.660	0.023	1.017	0.0954
2	0.683	0.607	0.590	0.017	1.158	0.111
3	0.607	0.539	0.524	0.015	1.234	0.112
4	0.539	0.378	0.356	0.022	2.237	0.299
5	0.378	0.255	0.242	0.013	2.802	0.325
6	0.255	0.173	0.148	0.025	3.393	0.322
7	0.173	0.113	0.094	0.019	4.301	0.347
8	0.113	0.070	0.053	0.017	5.611	0.380
					Total Strain	2.378
9	0.070	0.046	0.025	0.021	6.795	0.350
					Total Strain	2.798

**Table 8. 350°C PROCESSED UNREINFORCED ALUMINUM**

Roll #	T <sub>o</sub> (in)	T <sub>f</sub> (in)	Mill Gap Setting (in)	Mill Deflect. (in)	$\dot{\epsilon}$ (1/sec)	e (in/in)
1	0.746	0.660	0.640	0.020	1.134	0.116
2	0.660	0.585	0.570	0.015	1.189	0.113
3	0.585	0.512	0.500	0.012	1.332	0.125
4	0.512	0.355	0.335	0.020	2.321	0.305
5	0.355	0.239	0.220	0.019	2.901	0.327
6	0.239	0.159	0.140	0.019	3.573	0.333
7	0.159	0.102	0.084	0.018	4.561	0.357
8	0.102	0.065	0.044	0.021	5.824	0.371
					Total Strain	2.440
9	0.065	0.040	0.020	0.020	7.398	0.380
					Total Strain	2.926

**Table 9. 500°C PROCESSED ALUMINA COMPOSITE**

Roll #	T <sub>o</sub> (in)	T <sub>f</sub> (in)	Mill Gap Setting (in)	Mill Deflect. (in)	$\dot{\epsilon}$ (1/sec)	e (in/in)
1	0.755	0.678	0.660	0.018	1.048	0.101
2	0.678	0.605	0.590	0.015	1.145	0.108
3	0.605	0.534	0.524	0.010	1.265	0.117
4	0.534	0.373	0.356	0.017	2.252	0.300
5	0.373	0.256	0.242	0.014	2.780	0.317
6	0.256	0.171	0.148	0.023	3.428	0.329
7	0.171	0.113	0.094	0.019	4.245	0.336
8	0.113	0.073	0.053	0.020	5.445	0.361
					Total Strain	2.336
9	0.073	0.046	0.025	0.021	6.895	0.372
					Total Strain	2.798

**Table 10. 500°C PROCESSED UNREINFORCED ALUMINUM**

Roll #	T <sub>o</sub> (in)	T <sub>f</sub> (in)	Mill Gap Setting (in)	Mill Deflect. (in)	$\dot{\epsilon}$ (1/sec)	e (in/in)
1	0.746	0.655	0.640	0.02	1.165	0.122
2	0.655	0.589	0.570	0.019	1.125	0.101
3	0.589	0.513	0.500	0.013	1.344	0.128
4	0.513	0.351	0.335	0.016	2.371	0.317
5	0.351	0.233	0.220	0.013	2.953	0.334
6	0.233	0.157	0.140	0.017	3.587	0.328
7	0.157	0.104	0.084	0.020	4.446	0.338
8	0.104	0.066	0.044	0.022	5.713	0.365
					Total Strain	2.425
9	0.066	0.041	0.020	0.021	7.330	0.379
					Total Strain	2.901

**APPENDIX B**  
**HARDNESS TABLES**

Tables 11 and 12. AGING HARDNESS VERSUS TIME

	AGE DATA TABLE #1					(min)				
					Time					
Temp	30	60	600	1440	2000	4000	6000	8000	10385	
	51.2	64.2	78.5	84.6	88.3	69.6	54.7	45.2	51	
135°c	45.9	65.3	76.8	81.2	90.2	69.3	66.8	90.3	85.3	
	70.8	89.3	97	86.2	64.8	46.3	74	69.3	61	
	78.6	88.3	98	99	94.7	94.5	94	93	92.5	
	59.2	69.2	91.3	91	88	83.3	54.7	44.3	58.7	
150°c	62.3	73.8	90.3	93	89.5	69.7	85.5	90.3	87.7	
	66	81	95.4	95.9	71.6	63.5	51	56.5	64.7	
	80.6	84.5	96	97.9	97.3	98	94.8	94	95	

	AGE DATA TABLE #2									
				Time	(min)					
Temp	5	20	45	120	400	750	1000	2500		
	46.6	80	81.4	90.8	44	26	56	44.2		
175°c	38	83.3	88	89.6	67.7	69.8	81	87.5		
	48.9	93.3	96.8	103.1	46.5	67	73	46.3		
	62.3	94.8	92	96	87.7	97	96	92.8		
	54.5	71.8	81.6	88.5	34	89.5	79.3	91.6		
200°c	55.1	57.8	85.5	91.3	82	86	74.8	81.8		
	66.3	84.6	86.8	91	46.5	67	73	46.3		
	63.2	83.9	93.8	98.7	86.7	84.5	88.3	87.4		

Aging response for 135°C

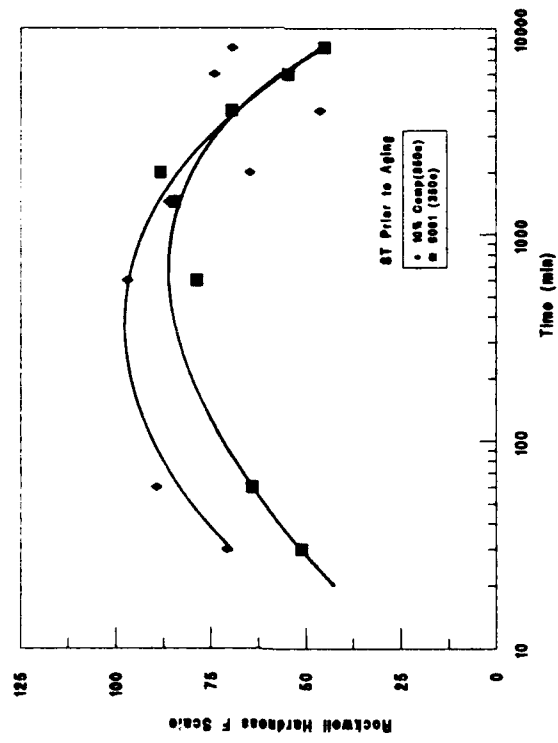


Figure 35. Aging response for material processed 350°C, and aged 135°C.

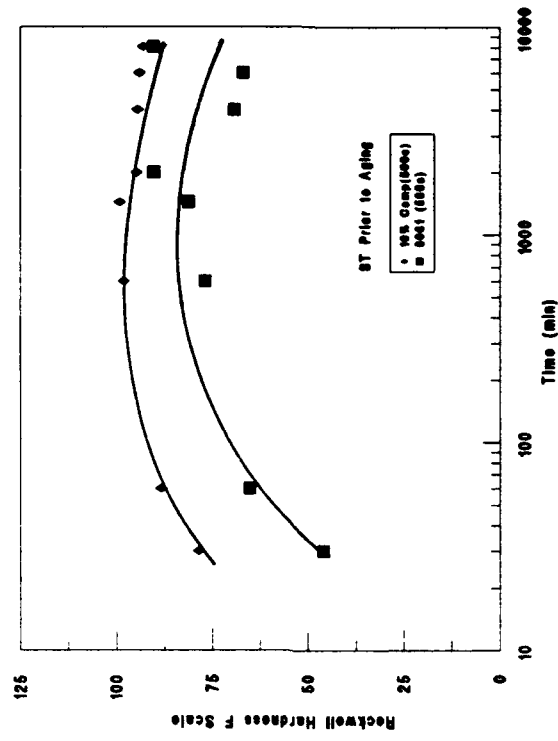


Figure 36. Aging response for material processed 500°C, and aged 135°C.

Aging response for 150°C

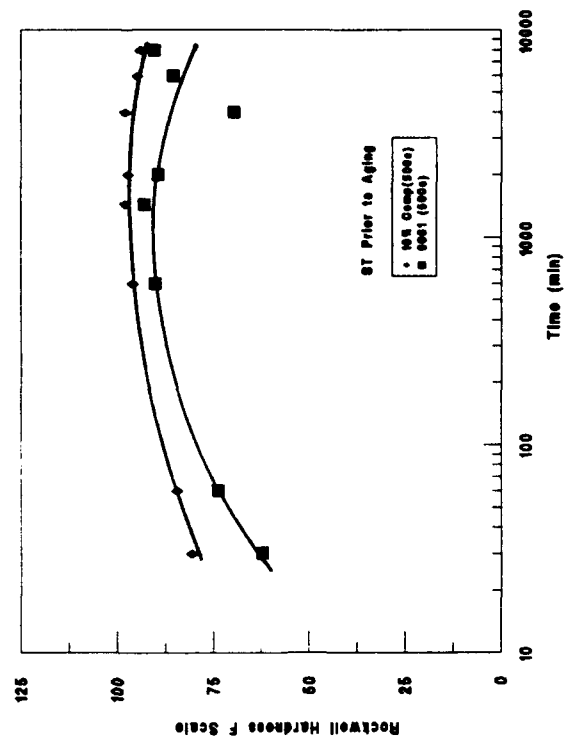


Figure 38. Aging response for material processed 500°C and aged 150°C.

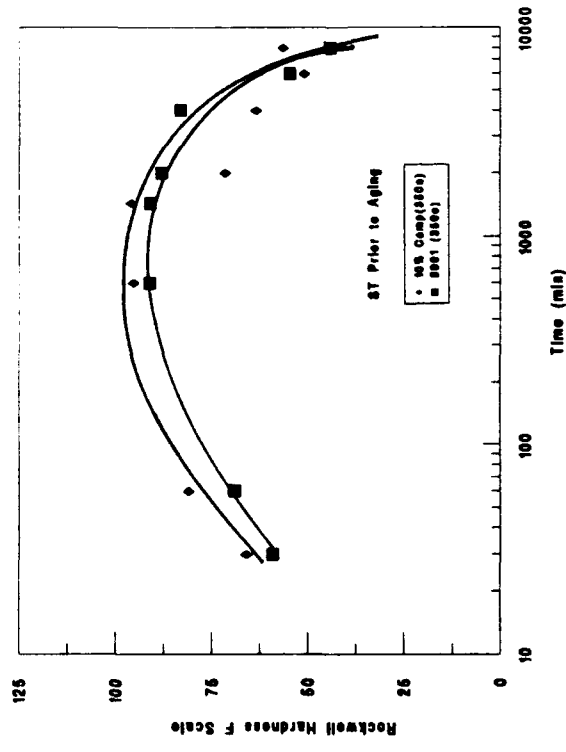
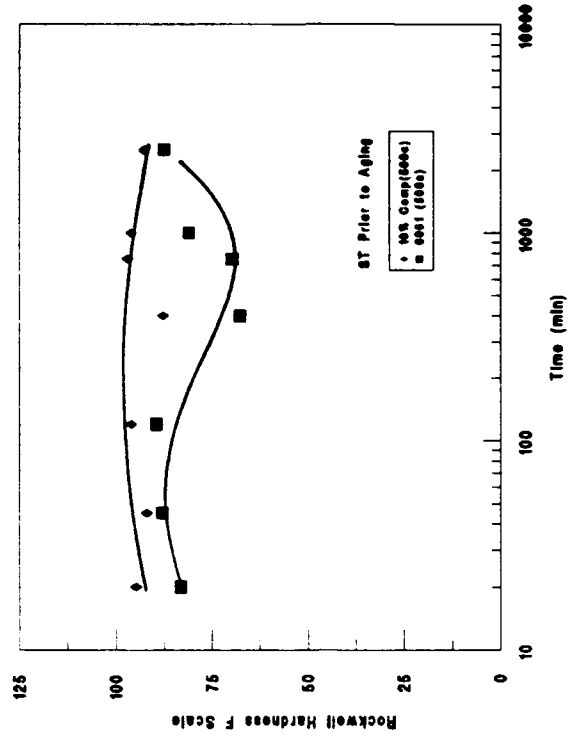
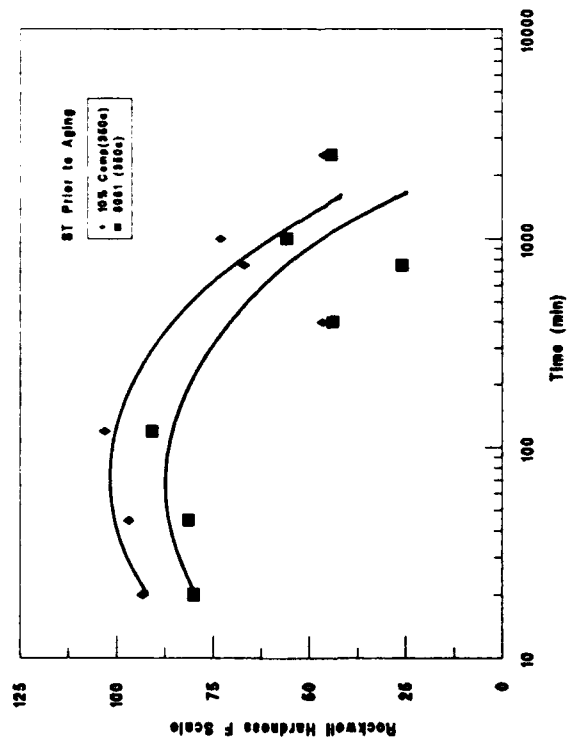


Figure 37. Aging response for material processed 350°C and aged 150°C.

**Aging response for 175°C**



**Figure 39. Aging response for material processed 350°C and aged 175°C.**



**Figure 40. Aging response for material processed 500°C and aged 175°C.**

**Aging response for 200°C**

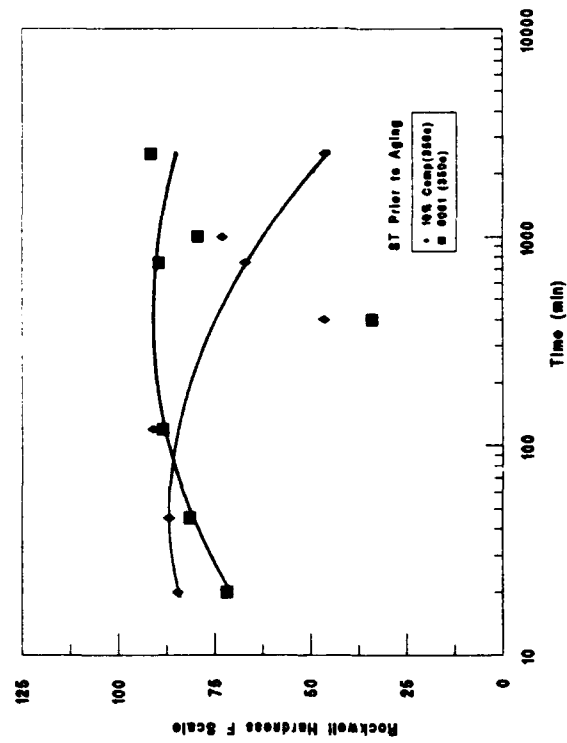


**Figure 41. Aging response for material processed 350°C and aged 200°C.**

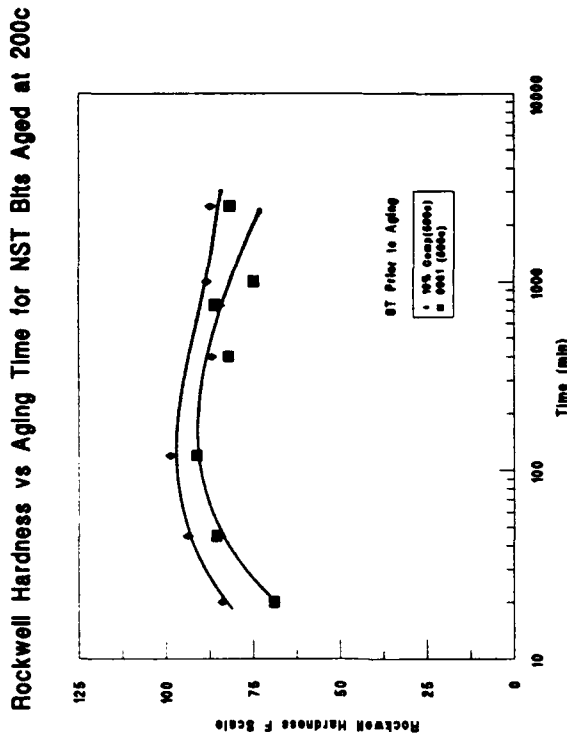


**Figure 42. Aging response for material processed 500°C and aged 200°C.**

APPENDIX C  
AGING INSTRON DATA  
MATERIAL PROCESSED AT 135°C

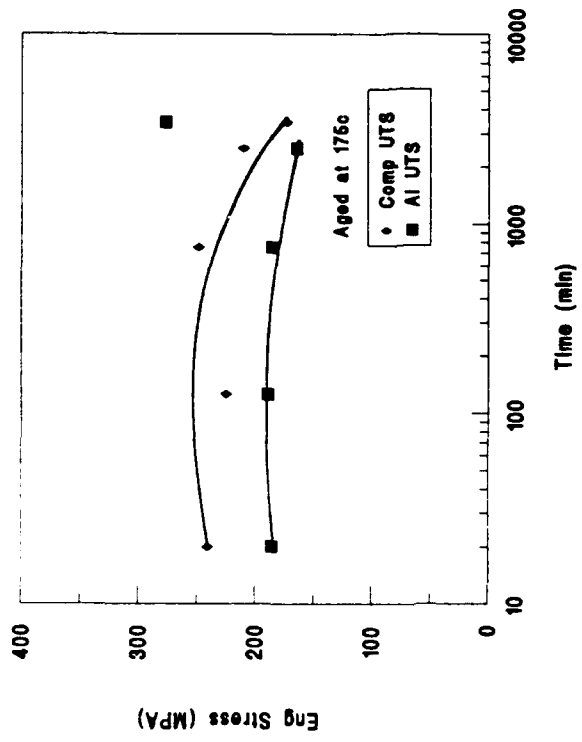


Figure 44. UTS for composite aged at 135°C.

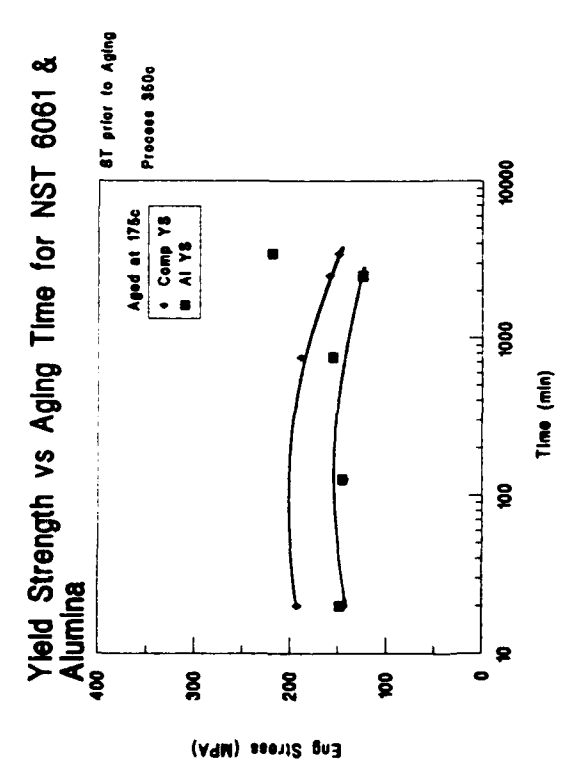


Figure 43. Yield strength for the composite aged at 135°C.

Yield Strength vs Aging Time for NST 6061 & Alumina

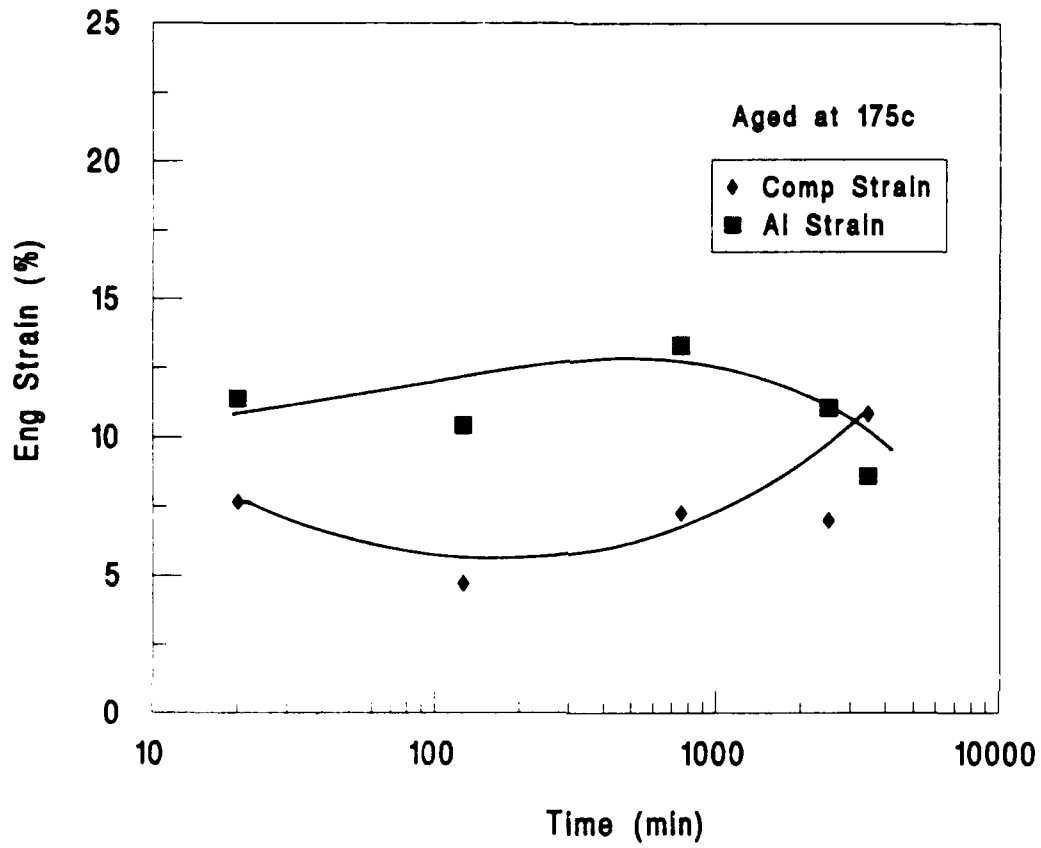


Figure 45. Elongation composite aged at 135°C.

## LIST OF REFERENCES

1. Taya, Minoru and Arsenault, Richard J., *Metal Matrix Composites Thermomechanical Behavior*, p. 1, Pergamon Press, 1989.
2. Meyers, M. A., and Chawla, K. K., *Mechanical Metallurgy: principles and applications*, p. 438, Prentice-Hall, 1984.
3. Taya, Minoru and Arsenault, Richard J., *Metal Matrix Composites Thermomechanical Behavior*, p. 1-2 Pergamon Press, 1989.
4. Meyers, M. A., and Chawla, K. K., *Mechanical Metallurgy: principles and applications*, p. 439, Prentice-Hall, 1984.
5. McNelley, T. R., and Kalu, P. N., "The Effects of Thermomechanical Processing on the Ambient Temperature Properties and Aging Response of a 6061 Al-Al<sub>2</sub>O<sub>3</sub> Composite", *Scripta METALLURGICA et MATERIALIA*, Vol. 25, pp. 1041-1046, Pergamon Press, 1991.
6. Humphreys, F. J., et al., "Microstructural development during thermomechanical processing of particulate metal-matrix composites", *Materials Science Technology*, Vol. 6, pp. 1157-1166, November 1990.
7. Taya, Minoru and Arsenault, Richard J., *Metal Matrix Composites Thermomechanical Behavior*, p. 3-5, Pergamon Press, 1989.
8. *Engineering Materials Handbook: composites*, Vol. 1, pp. 903-910, ASM International, 1987.
9. Gorsuch, T. E., *The Roles of Strain and Reheating Interval in the Continuous Recrystallization During Thermomechanical Processing by Warm Rolling of an Al-Mg Alloy*, Master's Thesis, Naval Postgraduate School, p. 11, December 1989.
10. Schaefer, T. A., *Thermomechanical Processing and Ambient Temperature Properties of a 6061 Aluminum 10 Volume Percent Alumina Metal Matrix Composite*, Master's Thesis, Naval Postgraduate School, p. 13, March 1990.
11. Macri, P.D., *Processing Microstructure and Elevated Temperature Mechanical*

*Properties of a 6061 Aluminum-Alumina Metal Matrix Composite*, Master's Thesis, Naval Postgraduate School, p. 12, December 1990.

12. Magill, M. D., *The Influence of Thermomechanical Processing Parameters on the Elevated Temperature Mechanical Behavior of a 6061 Aluminum-Alumina Metal Matrix Composite Materials*, Master's Thesis, Naval Postgraduate School, p. 23, December 1990.

13. Schauder, T. J., *The Elevated Temperature Behavior of a 10% Volume Al-Al<sub>2</sub>O<sub>3</sub> Metal-Matrix Composite*, Master's Thesis, Naval Postgraduate School, p. 24, March 1992.

14. P. N. Kalu and T. R. McNelly, "Microstructural Refinement by Thermomechanical Treatment of a Cast and Extruded Al-Al<sub>2</sub>O<sub>3</sub> Composite", *Scripta METALLURGICA et METERIALIA*, Volume 25, pp. 853-858, 1991.

15. Dieter, George, *Mechanical Metallurgy, 2nd Edition*, (International Student Edition), p. 633, McGraw Hill, 1976.

16. Schaefer, T. A., *Thermomechanical Processing and Ambient Temperature Properties of a 6061 Aluminum 10 Volume Percent Alumina Metal Matrix Composite*, Master's Thesis, Naval Postgraduate School, p. 4, March 1990.

17. *Metals Handbook, Tenth Edition*, Volume 2, edited by Davis, Joseph R., et al., pp. 4, 103-104, ASM International, 1990.

18. Mondolfo, L. F., *Aluminum Alloys: Structures and Properties*, p. 567, Butterworths, 1976.

19. Humphreys, F. J., et al., "Microstructural development during thermomechanical processing of particulate metal-matrix composites", *Materials Science Technology*, pp. 1160, Vol. 6, November 1990.

20. Askeland, D. R., *The Science of Engineering Materials*, Second Edition, p. 134, PWS-Kent, 1989.

21. Humphreys, F. J., et al., "Microstructural development during thermomechanical processing of particulate metal-matrix composites", *Materials Science Technology*, Vol. 6, pp. 1157, November 1990.

22. Humphreys, F. J. and Kalu, P. N., *Acta Metall.*, Vol 35, No. 12, pp. 2815-2829,

Perganon, 1987. and Kalu, P. N., and Humphreys, F. J., in *Aluminum Technology*, p. 197, Inst. Metals, 1986.

23. Humphreys, J. J., et al., "Microstructural development during thermomechanical processing of particulate metal-matrix composites", *Materials Science Technology*, Vol. 6, p. 1157, Vol. 6, November 1990.

24. Schaefer, T. A., *Thermomechanical Processing and Ambient Temperature Properties of a 6061 Aluminum 10 Volume Percent Alumina Metal Matrix Composite*, Master's Thesis, Naval Postgraduate School, pp. 13-15, March 1990.

25. Ashby, F.J., *Philos. Magazine*, Vol. 21, p. 399, 1970.

26. Porter, J. R., and Humphreys, F. J., *Met. Sci.*, Volume 13, p. 83, 1989.

27. Humphreys, F. J., and Kalu, P. N., *Acta Metall. Mater.*, Volume 38, p. 917, 1990

28. Hirsch, P. B., and Humphreys, F. J., *Physics of Strength and Plasticity*, A. S. Argon (ed.), MIT Press, p. 189, Cambridge, 1969.

29. Meyers, M. A., and Chawla, K. K., *Mechanical Metallurgy: principles and applications*, p. 423, Prentice-Hall, 1984.

30. Meyers, M. A., and Chawla, K. K., *Mechanical Metallurgy: principles and applications*, p. 421, Prentice-Hall, 1984.

31. Meyers, M. A., and Chawla, K. K., *Mechanical Metallurgy: principles and applications*, p. 421-2, Prentice-Hall, 1984.

32. Humphreys, F. J. et al, "Microstructural development during thermomechanical processing of particulate metal-matrix composites", *Materials Science Technology*, Vol. 6, pp. 1157-1158, Nov 1990.

33. Humphreys, F. J. et al, "Microstructural development during thermomechanical processing of particulate metal-matrix composites", *Materials Science Technology*, Vol. 6, pp. 1157-1158, Nov 1990.

34. Humphreys, F. J. et al, "Microstructural development during thermomechanical processing of particulate metal-matrix composites", *Materials Science Technology*, Vol. 6, pp. 1158-1159, Nov 1990.

35. Humphreys, F. J., "*International Conference on Recrystallization in Metallic Materials*", T. Chandra (ed.), p. 2, The Minerals, Metals & Materials Society, 1990.

36. Humphreys, F. J., et al., "Microstructural development during thermomechanical processing of particulate metal-matrix composites", *Materials Science Technology*, Vol. 6, pp. 1157-1166, November 1990.
37. Askeland, Donald R., *The Science of Engineering Materials*, 2nd Edition, p. 200, PWS Kent Publishers, 1989.
38. Humphreys, F. J., et al., "Microstructural development during thermomechanical processing of particulate metal-matrix composites", *Materials Science Technology*, Vol. 6, pp. 1160, November 1990.
39. Humphreys, F. J., et al., "Microstructural development during thermomechanical processing of particulate metal-matrix composites", *Materials Science Technology*, Vol. 6, pp. 1160, November 1990.
40. Askeland, Donald R., *The Science of Engineering Materials*, 2nd Edition, p. 571, PWS Kent Publishers, 1989.
41. Humphreys, F. J., et al., "Microstructural development during thermomechanical processing of particulate metal-matrix composites", *Materials Science Technology*, Vol. 6, pp. 1159, November 1990.
42. Humphreys, F. J., et al., "Microstructural development during thermomechanical processing of particulate metal-matrix composites", *Materials Science Technology*, Vol. 6, pp. 1160, November 1990.
43. Humphreys, F. J., et al., "Microstructural development during thermomechanical processing of particulate metal-matrix composites", *Materials Science Technology*, Vol. 6, pp. 1160, November 1990.
44. Schaefer, T. A., *Thermomechanical Processing and Ambient Temperature Properties of a 6061 Aluminum 10 Volume Percent Alumina Metal Matrix Composite*, Master's Thesis, Naval Postgraduate School, pp. 13-16, March 1990.
45. Schaefer, T. A., *Thermomechanical Processing and Ambient Temperature Properties of a 6061 Aluminum 10 Volume Percent Alumina Metal Matrix Composite*, Master's Thesis, Naval Postgraduate School, pp. 22-24, March 1990.
46. Humphreys, F. J., et al., "Microstructural development during thermomechanical processing of particulate metal-matrix composites", *Materials Science Technology*, Vol. 6, pp. 1160, November 1990.

47. Macri, P.D., *Processing Microstructure and Elevated Temperature Mechanical Properties of a 6061 Aluminum-Alumina Metal Matrix Composite*, Master's Thesis, Naval Postgraduate School, p. 17, December 1990.
48. Schaefer, T. A., *Thermomechanical Processing and Ambient Temperature Properties of a 6061 Aluminum 10 Volume Percent Alumina Metal Matrix Composite*, Master's Thesis, Naval Postgraduate School, pp. 20, March 1990.
49. Schauder, T. J., *The Elevated Temperature Behavior of a 10% Volume Al-Al<sub>2</sub>O<sub>3</sub> Metal-Matrix Composite*, Master's Thesis, Naval Postgraduate School, p. 45, March 1992.
50. Hertzberg, R. W., *Deformation and Fracture Mechanics of Engineering Materials*, Third Edition, pp. 254-256, Wiley, 1989.
51. Schaefer, T. A., *Thermomechanical Processing and Ambient Temperature Properties of a 6061 Aluminum 10 Volume Percent Alumina Metal Matrix Composite*, Master's Thesis, Naval Postgraduate School, pp. 20, March 1990.
52. Schauder, T. J., *The Elevated Temperature Behavior of a 10% Volume Al-Al<sub>2</sub>O<sub>3</sub> Metal-Matrix Composite*, Master's Thesis, Naval Postgraduate School, p. 36, March 1992.
53. *Metals Handbook*, Vol. 2, 10th ed., p. 104, ASM International, 1990.

## INITIAL DISTRIBUTION LIST

	No.Copies
1. Defense Technical Information Center Cameron Station Alexandria, VA 22304-6145	2
2. Library, Code 0142 Naval Postgraduate School Monterey, CA 93943-5002	2
3. Department Chairman, Code ME/Hy Department of Mechanical Engineering Naval Postgraduate School Monterey, CA 93943	1
4. Naval Engineering Curricular Office, Code 34 Naval Postgraduate School Monterey, CA 93943	1
5. Professor T. R. McNelley, Code 69MC Department of Mechanical Engineering Naval Postgraduate School Monterey, CA 93943	3
6. Professor P. N. Kalu, Code 69 Department of Mechanical Engineering Naval Postgraduate School Monterey, CA 93943	3
7. Lt. David F. Eastwood Jr., USN 313 Davis St. Portsmouth, RI 02871	2

8. Professor W. H. Kim, Code AS/KC  
Administrative Science Department  
Naval Postgraduate School  
Monterey, CA 93943

1